International Federation of Clinical Neurophysiology (IFCN) – EEG research workgroup: Recommendations on frequency and topographic analysis of resting state EEG rhythms. Part 1: Applications in clinical research studies

Claudio Babiloni [a,b,*], Robert J. Barry [c], Erol Başar [d], Katarzyna J. Blinowska [e], Andrzej Cichocki [f,g], Wilhelmus H.I.M. Drinkenburg [h], Wolfgang Klimesch [i], Robert T. Knight [j], Fernando Lopes da Silva [k], Paul Nunez [l], Robert Oostenveld [m], Jaeseung Jeong [n], Roberto Pascual-Marqui [o], Pedro Valdes-Sosa [p,q], Mark Hallett [r]

[a] Department of Physiology and Pharmacology "V. Erspamer", Sapienza University of Rome, Rome, Italy
[b] Hospital San Raffaele Cassino, Cassino, FR, Italy
[c] Brain & Behaviour Research Institute, and School of Psychology, University of Wollongong, Wollongong, NSW 2522, Australia
[d] Department of Neurosciences and Department of Neurology, Dokuz Eylül University Medical School, Izmir, Turkey
[e] Faculty of Physics, Department of Biomedical Physics, University of Warsaw, Warsaw, Poland
[f] Skolkovo Institute of Science and Technology (SKOLTECH), Moscow, Russia
[g] RIKEN AIP, Tokyo, Japan
[h] Janssen Research & Development, Janssen Pharmaceutica NV, Beerse, Belgium
[i] Centre for Cognitive Neuroscience, University of Salzburg, Salzburg, Austria
[j] Department of Psychology, University of California, Berkeley CA 94720-1650, CA, USA
[k] Swammerdam Institute for Life Sciences, University of Amsterdam, the Netherlands
[l] Cognitive Dissonance LLC, Encinitas, CA 92024, USA
[m] Donders Institute for Brain, Cognition and Behaviour, Radboud University, Nijmegen, the Netherlands
[n] Department of Bio and Brain Engineering, Program of Brain and Cognitive Engineering, Korea Advanced Institute of Science and Technology (KAIST), Daejeon, South Korea
[o] The KEY Institute for Brain-Mind Research, University of Zurich, Switzerland
[p] Key Laboratory for Neuroinformation of Ministry of Education, Center for Information in Biomedicine, University of Electronic Science and Technology of China, UESTC Chengdu, China
[q] Cuban Neuroscience Center (CNEURO), Playa, La Habana, Cuba
[r] National Institute of Health (NIH), National Institute of Neurological Disorders and Stroke (NINDS), Human, Motor Control Section, Medical Neurology Branch, Bethesda, USA

ARTICLE INFO

HIGHLIGHTS

- An IFCN Workgroup supplies recommendations on EEG frequency and topographical analysis for research.
- EEG recording, visualization, and extraction/interpretation best features are proposed.
- Pros and cons for clinical research of those features are discussed in light of controversies.

ABSTRACT

In 1999, the International Federation of Clinical Neurophysiology (IFCN) published "IFCN Guidelines for topographic and frequency analysis of EEGs and EPs" (Nuwer et al., 1999). Here a Workgroup of IFCN experts presents unanimous recommendations on the following procedures relevant for the topographic and frequency analysis of resting state EEGs (rsEEGs) in clinical research defined as neurophysiological experimental studies carried out in neurological and psychiatric patients: (1) recording of rsEEGs (environmental conditions and instructions to participants; montage of the EEG electrodes; recording settings); (2) digital storage of rsEEG and control data; (3) computerized visualization of rsEEGs and

control data (identification of artifacts and neuropathological rsEEG waveforms); (4) extraction of "synchronization" features based on frequency analysis (band-pass filtering and computation of rsEEG amplitude/power density spectrum); (5) extraction of "connectivity" features based on frequency analysis (linear and nonlinear measures); (6) extraction of "topographic" features (topographic mapping; cortical source mapping; estimation of scalp current density and dura surface potential; cortical connectivity mapping), and (7) statistical analysis and neurophysiological interpretation of those rsEEG features. As core outcomes, the IFCN Workgroup endorsed the use of the most promising "synchronization" and "connectivity" features for clinical research, carefully considering the limitations discussed in this paper. The Workgroup also encourages more experimental (i.e. simulation studies) and clinical research within international initiatives (i.e., shared software platforms and databases) facing the open controversies about electrode montages and linear vs. nonlinear and electrode vs. source levels of those analyses.

Contents

1. Introduction

In clinical research, resting state electroencephalographic (rsEEG) rhythms are often recorded from the patient's scalp during short (i.e., minutes) eyes-closed and -open conditions. This research mainly focuses on abnormalities in the frequency and topographical features of rsEEG rhythms to unveil neural dysfunctions in the regulation of quiet wakefulness in psychiatric and neurological diseases. Vigilance dysregulations may affect the

selectivity and efficiency of several higher cognitive functions such as attention (i.e., focused, sustained, selective or reflexive), episodic memory (i.e., encoding and retrieval of autobiographical events), and executive frontal functions (i.e., working memory and inhibitory control).

In 1999, the International Federation of Clinical Neurophysiology (IFCN) published the Guidelines entitled "*Recommendations for the Practice of Clinical Neurophysiology: Guidelines of the IFCN*" (EEG Suppl. 52, Editors: G. Deuschl and A. Eisen). These Guidelines

included the Chapter 1.4 entitled "*IFCN Guidelines for topographic and frequency analysis of EEGs and EPs*" (Nuwer et al., 1999), which revised the most mature techniques for the recording, storage, and subsequent topographic and frequency analysis of scalp rsEEG rhythms and evoked potentials (EPs). Since 1999, many new techniques and procedures for the topographic and frequency analysis of scalp rsEEG rhythms have become available in the public domain[1] or in the market for clinical research (Baillet et al., 2011).

The present position paper reports the recommendations of a Workgroup of field experts in frequency and topographic analysis of rsEEG rhythms as an update for the clinical research of the mentioned IFCN Guidelines (Nuwer et al., 1999). In the present paper, the concept of "clinical research" is defined as the ensemble of experimental studies carried out in patients with neurological and psychiatric diseases using the analysis of frequency and spatial features of rsEEG rhythms to unveil neurophysiological correlates of those diseases during their detection, natural evolution, and treatment. Noteworthy, the terms and methodological procedures discussed in this paper may not correspond to those used in the daily medical practice supplied in services of Clinical Neurophysiology, and we do not recommend that neurologists and psychiatrists should necessarily use the present terms and methodological procedures in that practice for diagnostic, prognostic or monitoring purposes. In other words, this paper is not a collection of guidelines for the application of techniques of Clinical Neurophysiology in daily medical practice.

In this paper, the Workgroup presents unanimous recommendations on the following procedures relevant for the rsEEG topographic and frequency analysis in clinical research: (1) recording of rsEEGs; (2) digital storage of rsEEG and control data; (3) computerized visualization of rsEEGs and control data; (4) extraction of rsEEG features in frequency and spatial domains, and (5) statistical analysis and neurophysiological interpretation of those rsEEG features. In the revision of those methodological aspects, the Workgroup briefly introduces some theoretical concepts and controversies about the generation of scalp rsEEG rhythms (i.e., determinism/randomness, linearity/nonlinearity, stationarity/nonstationarity) as a basis for a judicious use of new techniques of their frequency and topographical analysis. The choice of the techniques of interest was based on the consensus of all co-Authors on two main criteria: (1) the use by independent research groups in the field of Clinical Neurophysiology resulting in consistent results and (2) the production of insights in the neurophysiological mechanisms underlying psychiatric or neurological diseases. In some cases, earlier studies are mentioned to represent the Workgroup theoretical position about those techniques. The choice of those studies was not derived from a systematic and structured literature review as those following the procedural indications of the Institute of Medicine, Oxford (U.K.), or other clinical guidelines authorities.

Any techniques, procedures, or tools not explicitly mentioned in the following sections should not be considered as unreliable or only partially reliable. They may be entirely valid in limited experimental or clinical contexts, or only not yet widely used.

The Workgroup acknowledges that this paper reports relevant contents from the following papers: (1) "Committee report: publication guidelines and recommendations for studies using electroencephalography and magnetoencephalography" produced by the Society for Psychophysiological Research (Keil et al., 2014); (2) "Best practices in data analysis and sharing in neuroimaging using MRI" by the OHBM Committee on Best Practice in Data Analysis and Sharing (Nichols et al., 2017); (3) "Guidelines for the recording and evaluation of pharmaco-EEG data in man" produced by the International Pharmaco-EEG Society (IPEG; Jobert and Wilson, 2012); (4) "Guidelines and consensus statements" reported by the American Clinical Neurophysiology Society (ACNS) in https://www.acns.org/practice/guidelines; and (5) Guidelines of the IFCN such as "A revised glossary of terms most commonly used by clinical electroencephalographers and updated proposal for the report format of the EEG findings. Revision 2017" (Kane et al., 2017), "Standardized computer-based organized reporting of EEG: SCORE – Second version" (Beniczky et al., 2017), "IFCN standards for digital recording of clinical EEG. International Federation of Clinical Neurophysiology" (Nuwer et al., 1998), and "The standardized EEG electrode array of the IFCN" (Seeck et al., 2017). This paper also kept some still valid recommendations of the original IFCN Guidelines by Nuwer et al. (1999).

2. Recording of scalp rsEEG rhythms for topographic and frequency analysis

2.1. Preliminary assessment of subject's condition

Firstly, a few days prior to the recording of rsEEG rhythms, subjects should be instructed to have regular sleep on the night before that recording. Subjects should also be instructed not to use psychoactive substances and medications (i.e., foods and drinks including nicotine, caffeine, alcohol, and other stimulants in any form in the morning of the experiment). Subjects may take their psychoactive medication (i.e., benzodiazepines, antidepressant, etc.) normally the day before the EEG recording but not in the morning of that recording (the decision for this act should obviously be agreed after proper clinical consultation). It is assumed that such a short withdrawal of medications should be insufficient to cause therapeutic discontinuation problems and should allow harmonizing the assumption of the therapeutic regimen in all subjects enrolled without generating a truly unmedicated condition. However, the following issues should be considered. In such circumstances, residual effects of benzodiazepines or other psychoactive medications should be expected. For example, residual effects on the rsEEG activity may occur the next day. Furthermore, the residual drug agents may cause increased rsEEG beta rhythms and other effects on the next day. Moreover, a patient dependent on certain medications may experience some psychophysiological state changes due to a delay in taking medications that day, thus causing such personal effects as anxiety or early drowsiness. These factors should be annotated in the general subject's assessment before the rsEEG recording and taken into considerations in statistical models as confounding variables. These aspects should be properly reported and discussed in related publications.

Secondly, the preferred time for the recording of rsEEG rhythms is the morning after a satisfying light breakfast.

Thirdly, a brief interview of the subjects should confirm the standard subjects' quality of sleep during the night preceding the recording and the above conditions. If negative, the recording should be postponed to another date.

For more details, see the excellent IPEG (International Pharmaco-EEG Society) Guidelines by Jobert and Wilson (2012).

2.2. Environmental conditions

Recording of rsEEG rhythms is an experiment in the Clinical Neurophysiology of vigilance and should meet the following conditions.

---

[1] Popular WEB-based academic freeware platforms for EEG-MEG data analysis were systematically reviewed in Baillet et al. (2011) https://www.hindawi.com/journals/cin/2011/972050.

- First, a quiet and dimly lighted room.
- Second, acoustic noise should be negligible in the recording chamber.
- Third, the subject should rest on a comfortable half reclined armchair or bed.
- Fourth, the wall in front of him/her should be painted with a uniform light color (e.g., white, very pale yellow or green) with only a central fixation target at the height of his/her eyes.

2.3. Instructions to subjects

Three resting state conditions are typically used. Two of them are described in detail in the IPEG Guidelines for pharmaco-EEG recordings (Jobert and Wilson, 2012).

The first condition tests the neurophysiological mechanisms keeping the state of low vigilance with eyes-closed for several minutes (i.e., 5–15 min). It also probes the transition to drowsiness and sleep, hence the experimenter (or trained technologist) should *not* alert the subject in case of sleep. The instructions invite the subject to sit quietly, stay relaxed in a state of mind wandering (i.e., no goal-oriented mental activity), and keep the eyes closed. If the subject does not follow the instructions, the experimenter will repeat them (for more details, see Jobert and Wilson, 2012; Beniczky et al., 2017).

The second condition tests the neurophysiological mechanisms regulating the increase and decrease in the vigilance level while opening and closing the eyes sequentially (i.e., 5–10 min). The periods of eyes-open and -closed in response to experimenter's cue are short (i.e., 1 min), and the sequence of eyes-open and – closed is repeated (i.e., 2–4 times). The instructions to the subject are like those of the first condition. The experimenter will have to alert the subject in case of sleep to have enough EEG data related to the proper mental state. If the subject does not follow the instructions, the experimenter will repeat them (for more details, see Jobert and Wilson, 2012; Beniczky et al., 2017).

The third condition tests the neurophysiological mechanisms underlying the *steady maintenance* of low vigilance at eyes closed (i.e., 3–5 min) and moderate vigilance at eyes open (i.e., 3– 5 min). The instructions to the subject are like those of the second condition.

In the above resting state conditions, instructions of the experimenter to the subject must be very precise and consistent over subjects. These instructions might be difficult for patients with compromised brain function and cognitive decline and/or behavioral disorders (e.g., patients with dementia due to Alzheimer's disease). Therefore, experimenters should pay attention to behavioral states of subjects during the rsEEG recording and take notes that will guide the rejection of EEG recording periods characterized by subjects' drowsiness and alerts (for more details, see Jobert and Wilson, 2012; Beniczky et al., 2017).

2.4. Montage of EEG electrodes for the topographical analysis

Temporal and spatial samplings should be substantially higher than the temporal (spectral) and spatial information content of rsEEG signals to avoid distortion of the low spatial frequencies due to aliasing. Therefore, the use of a given electrode montage depends upon assumptions about this content.

The IFCN Guidelines by Seeck et al. (2017) recommend the use of 75 up to 256 electrodes for scalp rsEEG recording in clinical research, especially for the localization of epilepsy sources (where 256 electrodes were claimed to enhance the localization accuracy of epileptic sources compared with 128 electrodes). We agree with the high spatial sampling of rsEEG rhythms in clinical research ($\geq$48–64 until 128–256 electrodes) and the montage scheme proposed in those Guidelines.

According to IFCN standards (Nuwer et al., 1998), digital recording of scalp rsEEG data is usually made with a single cephalic ground electrode and a referential montage using a single common electrode as a physical reference. The choice of the referential electrode location has important implications as it affects the amplitude and polarity of scalp EEG voltage. In this line, left earlobe (e.g., A1) is often used as a physical electrode reference while the right one (e.g., A2) is recorded separately for later off-line re-referencing to the average of A1 and A2 (Nuwer et al., 1998). Less often, another non-cephalic (i.e., nose) or a cephalic location is used as a physical reference. The off-line average of A1 and A2 supplies a reference symmetrical on the body midline and preserves the original phase of rsEEG rhythms recorded over the scalp. However, imbalance due to A1 and A2 impedance differences may topographically shift rsEEG rhythms. Furthermore, A1 can be affected by high-amplitude electrocardiographic (ECG) activity (i.e., QRS complexes), contaminating exploring (i.e., "active") electrodes distant from the left ear. Moreover, nose electrode reference can be affected by spike potentials generated by microsaccades (Yuval-Greenberg et al., 2008). Therefore, a good experimental practice is the use of montages with more than one referential electrode (and always a non-cephalic electrode) for off-line data analysis. Furthermore, experimenters should check for ear impedances and the presence of EKG activities in rsEEG signals before the start of the EEG recording.

2.5. Montage of other sensors for control data collection

For the control of eye movements (i.e., saccades) or blinking in clinical research, vertical and horizontal electro-oculographic (EOG) potentials should be recorded from bipolar electrode pairs placed around the dominant eye. Other EOG montages as well as infrared or optical eye tracking can be used for specific applications.

For the control of the subject's arousal and vital signs, EKG Einthoven's derivations (e.g., heart rate variability), hand skin conductance, and respiration sensor belt are used, while neck electromyographic (EMG) activity probes vigilance state (Barry et al., 2011).

For more details on the placement of EOG, EKG, and EMG electrodes and recording settings, see earlier IFCN Guidelines (Nuwer et al., 1998; Seeck et al., 2017).

2.6. Setting of rsEEG recording parameters

According to IFCN standards (Nuwer et al., 1998), rsEEG are sampled at $\geq$250[2] samples per second (Hz) and 12/14-bit resolution per sample with a resolution down to 0.5 µV (0.1 Hz and $\geq$60–70 Hz anti-aliasing passband filter at 256 Hz; Nilsson et al., 1993). Analog 50 or 60 Hz notch-reject filter or high-pass filter set at $\leq$1 should be set when off-line digital filters are not available. Interest in EEG activity up to 100 Hz implies the anti-aliasing filter to be higher than 100, and the sampling frequency to be 4 times the filter cut-off frequency. Electrode-to-electrode variability of the amplifier gain should be $\leq$1% on calibration pulses and bio-calibration comparisons. Additional noise (i.e., environmental such as residual AC power line, lighting, electronic equipment in the vicinity, etc.) in the recording of rsEEG activity from 0.5 to 100 Hz must be at most 2.0 µV, preferably $\leq$1.0 µV. Common mode rejection ratio should be at least 85 dB for each electrode and inter-electrode crosstalk should be $\leq$1%, i.e., 40 dB down or better. See also suggestions of

---

[2] While traditional Fast Fourier Transforms (FFTs) require 2^N samples per analysis epoch, modern Discrete Fourier Transforms do not, and an acceptable modern lower limit for Fourier analysis would be a sampling rate of 250 Hz if the interest is for EEG frequencies <60 Hz.

the International Pharmaco-EEG Society during pharmacological experimental manipulations (Jobert and Wilson, 2012). Calibrations with square wave signals should assess the range of frequencies, sensitivities, and types of quantitative tests performed at the beginning and the end of each recording session.

2.7. Control of rsEEG recording during the experiment

Short periods of EEG signals (few seconds) related to voluntary blinking, bite-down, saccades, and small head movements allow the characterization of the subject's main artifacts before the start of the experimental recording.

During the rsEEG recording, experimenters should limit communications to the subject, strictly ensuring his/her general relaxation. They should report these communications as experimental notes for later data analysis.

3. Storage of EEG and control data

According to IFCN standards (Nuwer et al., 1998), rsEEG and control data are stored for the long-term in magnetic and optical storage devices in line with local ethical protocols. The stored recording should include demographic, personal (i.e., education and occupational attainments relevant for the cognitive reserve), clinical, and any instrumental information (e.g., genetic polymorphisms potentially explaining interindividual variance[3]) relevant about the subject.

4. Visualization of EEG and control data

According to IFCN standards (Nuwer et al., 1998), visualization of the scalp EEG and control data is based on a computer or tablet monitor in clinical research. Standard software allows changing the electrode montages from referential to bipolar or common average reference, as well as fine manual regulation of all visualization parameters (i.e., amplitude, frequency filtering, and velocity of the polygraph data).

For a detailed description and referral of the scalp rsEEG waveforms and graphoelements in adults and children, see the IFCN Guidelines by Beniczky et al. (2017) updating the Standardized Computer-based Organized Reporting (SCORE) of EEG activity.

4.1. Preliminary data analysis

In clinical research, two experts should blindly perform the preliminary data analysis to define the artifact-free segments (i.e., epochs) of scalp rsEEG rhythms, and inter-rater variability in the artifact identification should be computed.

The choice of the EEG epoch length is a tradeoff. Concerning the frequency resolution, the longer the epoch, the higher the resolution (e.g., 1 s, 1 Hz; 2 s, 0.5 Hz, etc.). Furthermore, short rsEEG epochs of a few seconds can be considered stationary and analyzed with standard procedures of spectral analysis (see Section 5 for the concept of rsEEG *microstates* according to the Fingelkurts' theory; Fingelkurts and Fingelkurts, 2006, 2014). A length around 2–10 s is commonly used (Jobert and Wilson, 2012).

Instrumental artifacts are usually due to bad electrode-skin contact (e.g., high resistance), a loop between exploring and reference electrode due to sweat or conductive material, strong electric fields generated by external sources, magnetic fields of simultaneously acquired functional magnetic resonance imaging (fMRI), etc.

Biological artifacts include eye blinking, other eye movements (e.g., saccades, nystagmus, or roving eye movements), EKG or pulse activity related to the cardiac cycle, head and face muscular tension, head movements, etc.

Traditional preliminary data analysis is also devoted to the control of the subject's vigilance during the rsEEG recording. In this analysis, epochs of rsEEG rhythms showing signs of drowsiness (e.g., significant attenuation or slowing in frequency of posterior dominant alpha rhythms and an increase of theta rhythms) and sleep (e.g., K complexes and sleep spindles) should be rejected from the quantitative data analysis. Important information about the subject's vigilance state also relies on slow-rolling eye movements as revealed by EOG with a proper low-pass filtering. See the American Academy of Sleep Medicine (AASM) rules for the visual scoring of sleep onset in adults (Silber et al., 2007).

Preliminary data analysis can be semi-automatically performed by analytical algorithms that supply a tentative detection of instrumental and biological artifacts in the rsEEG waveforms. They also supply a tentative correction of some of those artifacts, particularly precise for blinking, eye movements, EKG or pulse activity related to the cardiac cycle[4]. Distortions due to simultaneous fMRI should be carefully removed as well.

Other analytical algorithms are used to detect scalp rsEEG waveforms related to sleep (K-complex, sleep spindles, slow waves, cyclic alternating pattern, etc.) or epilepsy (spikes, ripples, spike-wave complexes, etc.) automatically. However, there is no conclusive consensus about the validity of these algorithms, and IFCN Guidelines have not certified automatic reports based on these technologies. We recommend the use of such algorithms only with conservative exclusion criteria setting, followed by visual inspection by physicians trained in EEG interpretation (e.g., especially clinical neurophysiologists). Two or more independent experts' review of the results of these techniques is strongly recommended for reaching consensus.

4.2. Identification of pathophysiological rsEEG waveforms

Physicians trained in EEG interpretation should control for the presence of spikes, sharp waves, periodic discharges, triphasic waves, and intermittent slowing in the EEG activity, due to epileptic or non-epileptic processes. For more details, please find the Guidelines of the European Federation of Neurological Societies (EFNS; Waldemar et al., 2007), American Clinical Neurophysiology Society's Standardized Critical Care EEG Terminology (Hirsch et al., 2013), Diagnostic Recommendations of the Dementia with Lewy Bodies Consortium (McKeith et al., 2005, 2017), IFCN Guidelines of Beniczky et al., 2017, and the 7th edition of Niedermeyer's Electroencephalography: Basic Principles, Clinical Applications, and Related Fields (Part II and III; Schomer and Lopes da Silva, 2018).

---

[3] Interesting discussions about the relation between rsEEG rhythms and genetic polymorphisms of dopamine and acetylcholine metabolism can be found in Bodenmann et al., 2009; Guindalini et al., 2014; Veth et al., 2014; Dauvilliers et al., 2015.

[4] Mathematical core features include autoregressive models, independent component analysis, principal component analysis, artificial neural networks, and other learning machines. In brief, autoregressive models construct a model of the artifact, detect it in the rsEEG data, and remove it by (weighted) subtraction. Principal and independent component analyses decompose the recorded rsEEG data in uncorrelated or orthogonally independent components. An experimenter identifies the components mainly due to artifacts (e.g., blinking, eye movements, EKG, etc.), reconstructs the rsEEG data without the rejected components, and inspects the reconstructed rsEEG data to confirm (or not) the success of the procedure. Only artifact free rsEEG data should be used in the subsequent quantitative analysis. More details about the use of those procedures for specific artefacts of rsEEG signals can be found in Moretti et al., 2003 and https://sccn.ucsd.edu/~jung/Site/EEG_artifact_removal.html. For the online processing of artifacts during EEG recordings, the most advanced methods consist of using adaptive filters allowing online processing. Such methods have been successfully applied in the case of eye-related artifacts (see for example, He et al., 2004).

5. Frequency analysis of scalp rsEEG rhythms

5.1. Dimensions in the generation of scalp rsEEG rhythms

Scalp rsEEG rhythms derive from the summation at scalp electrodes of the oscillatory component of post-synaptic potentials generated in large masses of cortical pyramidal neurons (several squared centimeters; Nunez and Srinivasan, 2006; Srinivasan et al., 2007), this component being the *output* of the resting state cortical system. Frequency analysis aims to decompose the basic frequency bands forming the recorded rsEEG signals and relate them to brain general arousal and vigilance.

The main *inputs* to the large neural mass generating rsEEG rhythms may include afferents from other cortical neural masses as well as thalamocortical and *ascending reticular* neurons (Nunez and Srinivasan, 2006).

Those inputs and outputs are supposed to be linked by a mixture of processes in *deterministic-random* (i.e., stochastic), *linear-nonlinear*, *stationary-nonstationary,* and other dimensions. In clinical research, the frequency analysis of rsEEG rhythms specifically aims to clarify the impact of brain diseases and therapeutic interventions on these processes and dimensions.

In this theoretical framework, *determinism* (as opposed to *randomness*) means that defined inputs to and parameters of the mentioned brain system produce scalp rsEEG signals always showing the same characteristics. In this strict meaning, rsEEG does not reflect a pure determinism. For example, in a seminal study (Stam and Pijn, 1999), dominant rsEEG alpha rhythms showing waxing and waning features around 10 Hz could not be distinguished from filtered noise and a random process in 98.75% of the data considered.

Linearity (as opposed to nonlinearity) means that any linear combination of inputs to the mentioned brain system produces the same linear combination of scalp rsEEG signals, each of which would have been produced in isolation by a given input. When the mentioned brain system is modeled as a random linear system, amplitudes and phases across different rsEEG frequencies are formally assumed to be independent of each other. Note this may not be true in absolute terms in some cases. RsEEG rhythms may be approximated to a random linear system with a deviation to low-dimensional nonlinear deterministic behavior only in <5% of data in healthy subjects (Lopes da Silva et al., 1997; Stam and Pijn, 1999). In contrast, when these rhythms are modeled as generated by a random nonlinear system, their amplitudes and frequencies may show harmonic relationships in the bispectrum and bicoherence (Billings, 2013).

Stationarity (as opposed to *nonstationarity*) implies that the statistical properties of scalp rsEEG time series are constant over time. This is not the case when long rsEEG time series lasting several seconds to minutes are considered (Blanco et al., 1995). In short rsEEG epochs of a few seconds, two types of stationarity of rsEEG rhythms can be distinguished, namely the strong and the weak stationarity. The former implies that all the joint probability distributions do not change as a function of time. The latter is the most commonly used and entails that the mean, variance, and autocorrelation function (power spectra) of rsEEG rhythms are constant as a function of time. These *quasi-stationary* patterns of rsEEG rhythms can be analyzed by traditional linear procedures of frequency analysis (Kaplan et al., 2005; Nunez, 2000) to unveil operational *microstates* (few milliseconds to seconds) and *macrostates* (several seconds) of the brain system according to the Fingelkurts' theory (Fingelkurts and Fingelkurts, 2006, 2014). Noteworthy, the term "microstates" was first introduced by Dr. Dietrich Lehmann with another meaning (Lehmann et al., 1987). Dr. Lehmann posited that momentary rsEEG potential distributions can be decomposed over time in a sequence of short (i.e. seconds) quasi-stable topographical patterns of EEG voltages, each defined as a brain electrical microstate reflecting ongoing mental processes (Lehmann et al., 1987). Recent reviews have insightfully revised earlier evidence of alterations in Lehmann's microstates in some neuropsychiatric disorders and their relationship with cerebral networks derived from neuroimaging research (Khanna et al., 2015; Michel and Koenig, 2018).

For both clinical practice and research, frequency analysis should span the wide range of frequencies of scalp rsEEG rhythms, considering that scalp electrodes limit the measurement of high-frequency rsEEG rhythms generated by circumscribed cortical neural populations, as the scalp and skull act as a spatial filter. Sensible amplitude of scalp rsEEG activity due to relatively large cortical neural populations can be seen under 50 Hz in standard physiological conditions, while low-amplitude rsEEG activity at 100–250 Hz can be detected in scalp recordings in certain conditions (HFOs; Engel and Lopes da Silva, 2012). We recommend that rsEEG frequencies of interest are related to defined peaks in the spectrum of the rsEEG feature considered, as not all frequencies may reflect substantial neural processes (Lopes da Silva, 2013).

When the frequency analysis of scalp rsEEG rhythms is undertaken, many different procedures can be used. Here we arbitrarily considered two broad classes of features of scalp rsEEG rhythms derived from frequency analysis, named as "synchronization" and "connectivity" (Babiloni et al., 2016a). In a broad sense, "synchronization" features ideally probe spatially local cortical neural oscillatory activity, while "connectivity" ones refer to an inter-areal interdependence of such activity as phase or amplitude.

5.2. "Synchronization"

In general, *"synchronization"* refers to a process wherein some linear and/or nonlinear oscillatory components of a system adjust a given property of their activity over time, showing a collective behavior (Boccaletti et al., 2002).

In the context of scalp rsEEG rhythms, features of the "synchronization" class reflect the temporal dynamics of the synchronized activity in local cortical neural populations, showing a collective oscillatory behavior at a macroscopic spatial scale of a few centimeters[5]. In this regard, the perpendicular alignment of pyramidal neurons with respect to the surface of cerebral cortex as well as microscopic, mesoscopic, and macroscopic columnar structures of the cerebral cortex result in synchronized post-synaptic potentials showing an oscillatory behavior with phase, amplitude, and frequency features. Distributed populations of those neurons in the cerebral cortex are considered as the main source of scalp rsEEG rhythms in both resting and task conditions.

Well-known *linear* features of scalp rsEEG rhythms are phase, amplitude or power density of the oscillatory activity. The width of the power spectral density and the spatial distribution of rsEEG rhythms can be used as a measure of cortical neural synchronization in quiet wakefulness.

The most typical *nonlinear metrics* showing complexity or synchronization within the rsEEG rhythms are estimated from phase-based cross-frequency coherence, auto-mutual information, entropy, or dimensional complexity (Jeong et al., 1998a,b;

---

[5] This activity subtends a fluctuating balance of cortical neural synchronization and desynchronization over time (Pfurtscheller and Lopez da Silva, 1999). In the "synchronization" class, one can ideally include all linear and nonlinear features of the rsEEG rhythms recordable at a given scalp electrode or estimated in one cortical region of interest (ROI) with spatial characteristics for the generation of EEG at the scalp level. These features characterize the amplitude, frequency, periodicity, and complexity of the rsEEG rhythms at that place.

Jeong, 2004; Dauwels et al., 2010; Sohn et al., 2010; Yang et al., 2016).

In traditional clinical research, standard linear spectral frequency analysis of scalp rsEEG rhythms is based on Fast Fourier Transform (FFT) applied to artifact-free EEG epochs.[6] Alternative procedures are also available (Pascual-Marqui et al., 1988a,b). Among them, parametric autoregressive models are statistically helpful (AR; Isaksson et al., 1981; Blinowska and Zygierewicz, 2012). Two frequent applications of the EEG frequency analysis are (1) the band-pass filtering of scalp rsEEG waveforms in the preliminary analysis and (2) the computation of the rsEEG amplitude/power density spectrum in the primary data analysis.

5.2.1. Band-pass filtering of scalp rsEEG waveforms and identification of graphoelements

Band-pass filtering of scalp rsEEG waveforms is mainly performed to remove high-frequency components (due to external electromagnetic noise or muscle activity) for two main research purposes: (1) the control of the EEG quality using the evaluation of artifactual low-frequency (<8 Hz) signals due to blinking, eyes and head movements or bad electrode-skin contact; (2) the recognition of physiological and pathological EEG graphoelements.

Physiological EEG graphoelements related to quiet wakefulness are bursts of ample rsEEG oscillations at about 10 Hz during the eyes-closed condition (i.e., posterior alpha rhythms) and their disappearance during the eyes opening condition (i.e., the block of alpha rhythms). In healthy control subjects, rsEEG rhythms should present these graphoelements with a magnitude depending on subjects' age, brain integrity, and mental state during the recording, so these variables should be carefully matched in control subjects and patients (Barry and De Blasio, 2017; Gratton et al., 1992; Babiloni et al., 2010). For example, posterior alpha rhythms and alpha rhythm blocking may be attenuated in healthy seniors in

---

[6] The exact characteristics of EEG signals are, in general terms, unpredictable. This means that one cannot precisely foresee the amplitude of an EEG grapho-element or the duration of an EEG wave. Therefore, it may be said that an EEG signal is a realization of a random or stochastic process. It is important to note, however, that successive values of an EEG signal have, in general, a certain degree of dependence. This can be put in evidence by computing a time average, for one realization of an EEG signal, of the product of the signal and a replica of itself shifted by a certain time delay: this time average is called the auto-correlation function. Applying the Fourier Transform (FT) to the EEG auto-correlation function, one obtains a representation of the EEG signal in the frequency domain in the form of frequency power spectra or power spectral density (units: $\mu V^2/Hz$). In the case that one wishes to estimate the correlation between two EEG signals, the cross-correlation function can be similarly computed; the FT of which is the cross-power-spectrum. It is useful to use a normalized quantity derived from the cross-power spectrum, namely the coherence function to estimate the linear relationships between different EEG signals. Further, the counterpart of the coherence function is the phase function which can provide information about the time relations between EEG signals. The computation of power spectra can be speeded up by applying the Fast Fourier Transform (FFT) algorithm. In the data analysis, the FFT is preferably applied after multiplying by a "window" (Hanning window, Welch's method) to reduce the ends of the epoch to zero to avoid spectral leakage. In the case that the signals are not Gaussian, higher order spectra must be considered, namely the bi-spectrum that is obtained by applying a two-dimensional FT to one signal that can reveal the existence of phase coupling between different frequency components. Alternatively, one may estimate power spectra using parametric models, namely autoregressive models, or autoregressive moving average models, which are described by linear difference equations. These models allow a considerable EEG data reduction and are being used mainly in estimating transfer functions between EEG signals in the analysis of functional connectivity. An important problem in EEG analysis is that EEG signals can only be considered as stationary during relatively short epochs, which complicates the interpretation of analyses based on the application of FT. This problem can be reduced by using methods based on orthogonal sets of wavelets, i.e., waveform templates that usually have the form of damped oscillations. For the band-pass filtering of scalp rsEEG data, Finite Impulse Response (FIR) may be better than Infinite impulse response (IIR), characterized by a nonlinear phase (although much faster since recursive).

---

relation to a natural deterioration of projections from cholinergic basal forebrain (Wan et al., 2019).

Concerning pathophysiological EEG graphoelements, typical examples are (1) the prominent low-frequency waves at <8 Hz during quiet wakefulness in seniors with cognitive deficits and (2) spike-wave epileptic complexes and peculiar high frequency oscillations and ripples (>70 Hz) generated by epileptogenic zones in epileptic patients. In this line, some criteria and algorithms disentangling physiologic from pathologic scalp EEG high frequency oscillations and ripples are under scientific evaluation (Roehri and Bartolomei, 2019; Thomschewski et al., 2019).

The detection of these rsEEG graphoelements can be automated using thresholds based on time-frequency analysis of rsEEG rhythms or considering their time varying spectral content. In this line, a first critical aspect is the estimation of the trade-off between the time and frequency resolutions of that spectral analysis. For this purpose, several methodological procedures can be used, based on diverse a priori settings (Principe and Brockmeier, 2015; Chandran et al., 2016). Among them, the spectrogram (i.e., windowed Fourier transform) provides a uniform time-frequency resolution depending on the choice of the length of the rsEEG segments. Scalogram (i.e., wavelet transform) allows a higher temporal resolution for higher rsEEG frequencies. A few Wigner-derived distributions of the Cohen's class fit practically any setting of the mentioned constraints. However, all these settings need a priori decisions by experimenters about which functions can properly model expected rsEEG transients. In this respect, Gabor functions (i.e., Gaussian envelopes that are modulated by sinusoidal oscillations) are particularly useful as they can parametrically describe a large variety of rsEEG transients. Of note, suboptimal choices of Gabor functions can bias the reconstruction of time-frequency readouts.

Compared to the mentioned procedures of time-frequency analysis, matching pursuit decomposition presents at least two advantages (Mallat and Zhang, 1993). It allows an excellent time-frequency trade-off for the analysis of rsEEG segments and minimizes the arbitrary choice of a model of transient EEG activity (Durka and Blinowska, 1995). Indeed, matching pursuit decomposition iteratively and adaptively subtracts from the EEG signal its projection on "atoms" taken from a very wide and redundant dictionary of Gabor functions. Usually, Gabor functions are used since they provide the best time-frequency resolution. The resulting time-frequency features (amplitude, frequency, time occurrence and time span) can be used as inputs to the mathematical classifiers for research applications in epilepsy (Durka et al., 2005; Khlif et al., 2013; Z-Flores et al., 2016) and sleep (Malinowska et al., 2009; Durka et al., 2015). Furthermore, matching pursuit decomposition has been adapted for multivariate datasets and EEG source estimation (Durka et al., 2005; Bénar et al., 2009).

5.2.2. Computation of rsEEG amplitude/power density spectrum

The computation of the rsEEG amplitude/power density spectrum by linear procedures is a primary step of the data analysis. It allows the visualization of amplitude (μV) or power density ($\mu V^2/Hz$), frequency-bin-by-frequency-bin, for electrodes of interest.

Although the rsEEG frequency bands are universally referred to with the Greek letters (e.g., delta, theta, alpha, beta, and gamma), there are several different classifications about their frequency limits (Klimesch, 1999; Pfurtscheller and Lopes da Silva, 1999; Shackman et al., 2010; Lopes da Silva, 2011).

The IFCN Guidelines of Nuwer et al. in 1999 report two different classifications of the rsEEG frequency bands for delta, theta, alpha, beta, and gamma. The first classification is based on variable frequency bins within the bands and overlapping frequency limits across the bands. Instead, the second classification uses frequency

Table 1
Subdivision of the scalp-recorded resting state EEG rhythms in fixed frequency bands according to the Guidelines of International Federation of Clinical Neurophysiology (IFCN; Nuwer et al. 1999), International Pharmaco-EEG Society (IPEG; Jobert and Wilson, 2012), and IFCN Glossary of terms most commonly used by clinical electroencephalographers (Kane et al., 2017). Note that the Guidelines of IFCN by Nuwer et al. (1999) reported two alternative subdivisions (I and II).

Frequency (Hz)	IFCN 1999 (I)	IFCN 1999 (II)	IPEG 2012	IFCN-2017 Glossary
Delta	0.5–4	0.5–4	1.5–<6	0.1–<4
Theta	4–8	5–7	6–<8.5	4–<8
Alpha	α1: 8–10	8–12	α1: 8.5–<10.5	8–13
	α2: 10–12/13		α2: 10.5–<12.5	
Beta	β1: 12–16	β1: 14–20	β1: 12.5–<18.5	14–30
	β2: 16–20	β2: 21–30	β2: 18.5–<21	
	β3: 20–24		β3: 21.0–<30	
	β4: 24–28			
	β5: 28–32			
Gamma	γ1: 32–36	γ1: 30–40	30–<40	>30–80
	γ2: 36–40	γ2: 40–…	γ1: 30–<65[*]	
	γ3: 40–44		γ2: 65–<90[*]	
	γ4: 44–48		γ3: 90–<135[*]	
	…			

[*] Empirical subdivision.

bands characterized by 4-Hz intervals and non-overlapping frequency limits.[7]

In the literature, the beta range is extended in some cases to 30 Hz and other cases to about 35 Hz (Engel and Lopes da Silva, 2012). Above this, the frequency spectrum spans the gamma band. Gamma frequency sub-bands (gamma 1, gamma 2, etc.) of rsEEG rhythms range from 30 to 70 Hz. For components >70 Hz, the term high frequency oscillations (HFOs) is used. It is advisable to name the frequency range in parenthesis always and note whether the HFOs show a transient (burst-like) or continuous (steady-state) characteristic (Engel and Lopes da Silva, 2012).

The Guidelines of the IPEG report partially different frequency limits of delta, theta, alpha, beta, and gamma for pharmaco-rsEEG studies (Jobert and Wilson, 2012), based on previous investigations using spectral factor analysis. The limits of the fixed frequency bands overlap. For the higher frequencies empirically chosen, the following frequency ranges are suggested: 30–<65 Hz (gamma 1), 65–<90 Hz (gamma 2), and 90–<135 Hz (gamma 3) (see Footnote 7).

The IFCN Glossary of terms most commonly used by clinical electroencephalographers (Kane et al., 2017) reports another classification of the rsEEG frequency bands. In that classification, the limits of some fixed frequency bands overlap each other while others do not overlap.

Table 1 reports the subdivision in fixed frequency bands proposed in the Guidelines of IFCN (Nuwer et al., 1999; Kane et al., 2017) and IPEG (Jobert and Wilson, 2012). Considering this lack of consensus, we recommend the most recent IFCN and IPEG Guidelines for clinical research (Jobert and Wilson, 2012; Kane et al., 2017).

For some clinical research applications, the frequency analysis of scalp rsEEG rhythms can consider individual differences. For example, a clinical group may be characterized by a mean slowing in the peak frequency of alpha power without any substantial change in their amplitude. In this case, the use of fixed frequency bands would result in a statistical effect erroneously showing alpha amplitude/power density values lower in the clinical than the control group. This confound can be avoided considering the individual alpha frequency (IAF) peak, defined as the maximum amplitude/power density peak in the alpha range (Klimesch, 1999; Klimesch et al., 1998). An analysis on this individual basis would unveil a statistical effect showing IAF peak values lower in the clinical than the control group with no difference between the two groups in the alpha amplitude/power density.

For the mentioned individual frequency analysis of scalp rsEEG rhythms, two frequency landmarks may be considered: (1) the transition frequency (TF) between the theta and alpha bands and (2) the IAF peak (Klimesch, 1999; Klimesch et al., 1998; Klimesch, 2012, 2013). Based on the TF and IAF, delta, theta, and alpha frequency bands are defined as follows: delta from TF − 4 Hz to TF − 2 Hz, theta from TF − 2 Hz to TF, low-frequency alpha band (alpha 1 and alpha 2) from TF to IAF, and high-frequency alpha band (or alpha 3) from IAF to IAF + 2 Hz. The other bands are generally defined based on the above fixed frequency bands, as their frequency peaks cannot be unambiguously detected in many healthy and neurological subjects.

We recommend investigating topographical abnormalities of rsEEG power density/amplitude spectra in patients with brain diseases compared with healthy subjects. In healthy subjects, scalp rsEEG rhythms at different frequency bands show reference topographical distributions, underlying neurophysiological generating mechanisms and functions: (1) alpha 1 and 2 rhythms are prominent in sensory and posterior associative cortical regions; they may be associated with the endogenous regulation of brain arousal, thalamocortical flows of sensory information, and retrieval of stored semantic information from cerebral cortex (Klimesch et al., 2007; Başar, 2012; Fries, 2015); (2) beta 1, beta 2, and gamma rhythms are dominant in frontal areas; they may be associated with the regulation of thalamocortical flow of motor commands, imagery, and plans across basal ganglia and motor thalamus (Pfurtscheller and Lopes da Silva, 1999; Neuper et al., 2006; Oswal et al., 2013a,b); (3) delta and theta rhythms are mainly represented in associative frontal and posterior cortical regions; they might synchronize long-range and multi-functional brain regions, facilitating the generation of beta 2 and gamma rhythms during a variety of task-specific cognitive information processing (Canolty and Knight, 2010; Fries, 2015; Voytek and Knight, 2015; Helfrich and Knight, 2016); (4) these delta and theta rhythms may reflect the thalamocortical mechanisms underpinning the transition from wakefulness to sleep (Steriade, 2006) and the phase-locked low-frequency neurophysiological processes accompanying sensory and cognitive events. These low-frequency neurophysiological processes may play a key role in the formation

---

[7] Of note, this classification is quite similar to that obtained by Lopes da Silva in 2011 using a statistical factorial analysis of rsEEG spectral values. That analysis unveiled infra-slow at <0.2 Hz, delta from 0.2 to 3.5 Hz, theta from 4 to 7.5 Hz, alpha and mu from 8 to 13 Hz, beta from 14 to 30 Hz, gamma from 30 to 90 Hz, and high-frequency oscillations >90 Hz. In this case, the limits of the fixed frequency bands did not overlap each other.

of evoked or event-related potentials (Klimesch et al., 2007; Başar, 2013; Güntekin and Başar, 2016).

The computation of the scalp rsEEG amplitude/power density spectrum is performed for two main purposes in clinical research. The first purpose is a second-level control of the quality of those rsEEG epochs. A residual influence of eye blinking and movements is expected to produce increased amplitude/power density values in the delta-theta band of the frontal rsEEG activity. Furthermore, head and neck muscle activity may generate increased rsEEG amplitude/power density values at the frontal and temporal electrodes in a broad range of high frequencies. The general effect of those artifacts is a sort of *step* of amplitude/power density in frontal and temporal electrodes when compared with the other electrodes. In the presence of these artifactual spectral rsEEG features, the preliminary analysis of rsEEG epochs must be repeated.

After a correct removal of the rsEEG epochs contaminated by artifacts, a rsEEG amplitude/power density spectrum is expected to show the following physiological characteristic features: (1) a characteristic peak of the alpha amplitude/power density (8–12 Hz) in the resting condition with eyes closed and a reduction in alpha amplitude/power during the condition of resting state eyes open (These features can be less clear for neurological patients and healthy seniors); (2) an inverse relationship between the frequency bin and the amplitude/power density value from the rsEEG rhythms; namely, the higher the frequency bin, the lower the amplitude/power density value; and (3) the highest values of the delta and theta band in the frontal electrodes while the alpha rhythms are expected to achieve their highest values in the occipital electrodes.

The second purpose of the scalp rsEEG amplitude/power density computation is the extraction of quantitative markers from delta to gamma frequency bands associated with physiological and pathophysiological mechanisms of cortical neural synchronization. This analysis usually includes the operations of integrating, summing, or computing the ratio of the amplitude/power density values between specific frequency bands (e.g., delta, theta, alpha, and several beta and gamma bands). These frequency bands can have frequency limits equal for all subjects (i.e., fixed frequency bands), or those boundaries can be determined on an individual basis using anchor frequencies.

An interesting branch of the "synchronization" analysis from scalp rsEEG rhythms is represented by the computation of the so-called bispectrum at a given electrode or rsEEG source. This analysis unveils the intrinsic correlation between the phase of a low-frequency (e.g., delta or theta) rsEEG activity and that at higher (e.g., beta or gamma) rsEEG frequency. An important application of this procedure in clinical research concerns the study of the neurophysiological underpinning for monitoring the depth of anesthesia (Mukamel et al., 2011).

5.2.3. Absolute and relative rsEEG amplitude/power density

FFT outcome corresponds to the absolute amplitude/power density, measured in each frequency band. Relative amplitude/power density is, instead, evaluated as the ratio between the absolute amplitude/power density at a given frequency band (bin) and the sum or the mean of the amplitude/power density across all frequency bands (bins) of the scalp rsEEG spectrum (e.g., a good choice may be from 0.5 to 45 Hz; in any case, the frequency range used should be specified in the methodology section of papers). In some cases, the result of this normalizing operation is expressed as a percentage.

Hemispherical asymmetries of the amplitude (μV) or power density (μV^2/Hz) of scalp rsEEG rhythms are of interest as an enrichment biomarker in testing research hypotheses in patients with motor or language disorders, which typically show a dominance in the left hemisphere. Left-right asymmetries of these rsEEG variables are often evaluated by the asymmetry index (e.g., left minus right/left plus right), expressed as a percentage. This index has the advantage that its values run from -100% to $+100\%$. Other specific parameters are optional. Frequency content calculated in these ways is usually expressed as EEG amplitude values, in μV. Some users prefer to scale using power density instead of amplitude.

5.2.4. Nonlinear processes underlying rsEEG rhythms: How to test and measure them?

Although scalp rsEEG rhythms show prominent linear features (Lopes da Silva, 1994; Stam and Pijn, 1999; Blinowska and Zygierewicz, 2012), some brain diseases such as epilepsy (Pijn et al., 1997), schizophrenia (Kim et al., 2000), and neurodegenerative dementing disorders (Hernandez et al., 1996; Jeong et al., 1998a,b, 2001a,b; Stam, 2005) may induce detectable nonlinear rsEEG features to be better characterized in clinical research.

We think that the value of nonlinear procedures of scalp rsEEG data analysis may be better understood comparing more systematically nonlinear procedures in neurological patients and healthy controls. For this purpose, the following methodological approaches are of interest.

Nonlinear autoregressive moving average model with exogenous inputs (NARMAX) is a comprehensive approach to model scalp rsEEG rhythms in the time, frequency, and spatio-temporal domains as the outcome of a nonlinear brain system (Billings, 2013). In general, NARMAX may represent many nonlinear systems including those showing behaviors such as chaos, bifurcations, and subharmonics. In the past, it has successfully been used to provide measures of brain dynamics based on parametric and nonparametric methods (Hernandez et al., 1996; Valdes et al., 1999; David et al., 2006).

Another approach is based on Takens' Theorem (Takens, 1981). This theorem allows reconstructing dynamics of nonlinear systems by an embedding procedure, namely a sequence of observations (i.e., embedding values) of system states at proper discrete times (see an application to rsEEG features in Jeong et al., 1999). In general, the behavior of these systems can be described by the points of the embedding values as trajectories in the corresponding state space. These trajectories can converge to limit sets of the state space, called attractors. Of note, it should be stressed that to be valid, Takens' theorem requires that (1) dynamical systems examined be deterministic. This is not the case in the large majority of rsEEG epochs recorded in healthy subjects, which prominently show stochastic features (Lopes da Silva, 1994; Stam and Pijn, 1999); and (2) mathematical modeling takes into account formally if dynamics of the system and the mentioned observations are autonomous as opposed to be generated by another deterministic system (Stark et al., 2003). Keeping in mind these requirements, reliability and validity of Takens' theorem application on rsEEG research strictly depend on its correct formulation, based on the knowledge of all driving forces and deterministic or stochastic nature of the underlying nonlinear system. Unfortunately, this knowledge is not easily obtained as nonlinear behavior of deterministic and autonomous systems can be mimicked by stochastic and externally driven systems in some circumstances (Billings, 2013). Therefore, future research should enhance our ability to obtain that knowledge more precisely.

The mentioned attractors can show several features as a function of brain dynamics such as point attractors (linear system), limit cycles, chaos, and others, with the chaotic attractors having attracted a remarkable interest (for a review, see Faure and Korn,

2001; Korn and Faure, 2003). An attractor is called chaotic when the corresponding dynamic behavior is described by measures of its degrees of freedom by a non-integer, fractal dimension, correlation dimension, nonlinear parameters of Markov's processes, and positive Lyapunov exponents, using surrogate signals as a reference (Faure and Korn, 2001; Korn and Faure, 2003). Chaotic nonlinear systems are expected to show some typical behavior (e.g., self-similarity, self-organization, and sensitive dependence on initial conditions where small changes of control parameters may lead to large variations of the system state). In general, healthy subjects show limited rsEEG epochs subtending determinist nonlinear systems (Lopes da Silva, 1994; Stam and Pijn, 1999). In contrast, epileptic (especially ictal zone) and neurodegenerative dementing disorders point to a significant increase of features subtending nonlinear systems (Hernandez et al., 1996; Stam, 2005).

Finally, a popular approach is based on Information theory (Shannon, 1948). This theory provides basic concepts of mutual information and entropy to compute the bounds and capacity of neural information transfer underlying the generation of rsEEG rhythms (Jeong et al., 1998a,b, 2001a,b; Hlaváckóvá-Schindler et al., 2007). Specifically, the entropy of a random variable defines the average amount of information produced by a probabilistic stochastic source of data, while mutual information of two random variables measures the amount of information obtained about one random variable through the other random variable. The information-theoretical analysis may be of interest when rsEEG variables with potential clinical value (diagnostic, prognostic) are initially found to be multi-parametric (continuous parameters coexisting alongside discrete settings) and with nonlinear relations between the parameters (Jeong, 2004; Schwilden, 2006; Dauwels et al., 2010). If rsEEG variables show these features, the information-theoretical analysis may unveil a decreased complexity of rsEEG rhythms in relation to disease severity or progression. However, it should be remarked that entropy is just a measure, applicable to even linear systems (Kullback, 1959).

For fruitful clinical research applications, the following recommendations may be considered:

First, nonlinear measurements are inappropriate to analyze rsEEG rhythms generated by linear processes, so we recommend a preliminary evaluation of the linearity-nonlinearity dimension in the data to avoid ungrounded applications of those measurements.

Second, a deterministic nonlinear dynamical system may produce observable variables with apparent statistical random features. Furthermore, rsEEG rhythms may be generated by natural random fluctuations of linear or nonlinear systems. Therefore, the random-deterministic dimension of rsEEG time series examined should be carefully tested before nonlinear data analysis (Lopes da Silva et al., 1997; Kanz and Schreiber, 1997).

Third, the time delay, embedding dimension, noise, and the number of data samples substantially affect the outcome of nonlinear measurements derived from Takens' theorem (Takens, 1981). Therefore, they should be determined and cross-validated with extreme caution (for examples see Jeong et al., 1998a,b). When there is uncertainty about how to tackle the above error sources, linear measurements may be preferable even if nonlinearity (deterministic or stochastic) of the brain system appears from the data analysis, as one might approximate a parabolic function with several straight lines.

Fourth, results of nonlinear measurements may be biased by autocorrelation effects in rsEEG rhythms. A valid way to tackle

these effects it to discard vector pairs with time indices less than the autocorrelation time (Theiler, 1986).

Fifth, some nonlinear measures were found to be sensitive to relatively low levels (e.g., 5%) of colored or filtered noise in the data (Osborne and Provenzale, 1989; Kanz and Schreiber, 1997), so this aspect should be tested in the validation of new computational procedures.

Some non-exhaustive methodological suggestions to implement the above recommendations are reported in the following.

First, 10,000 or more data points in rsEEG signals (more than 3 min) with a proper sampling frequency may be considered a minimum requirement for the use of nonlinear measurements of attractors, information content etc. (Eckman and Ruelle, 1992; Stam and Pijn, 1999; Jeong, 2004; Stam, 2005). The same sampling and rsEEG power spectra should be imposed in the generation of surrogate linear stochastic time series as control data. Statistical differences of nonlinear measures between the real and surrogate rsEEG rhythms may suggest nonlinear determinism in the former (Theiler et al., 1992; Theiler and Rapp, 1996; Latchoumane and Jeong, 2011). We recommend that this procedure is repeated for more than 20 independent surrogate datasets with $p < 0.05$ corrected for multiple comparisons. However, it should be remarked that the use of the FFT with phase surrogates only tests against a linear stochastic alternative. It is not a test of general (possibly nonlinear) stochastic process against a deterministic process (see for a discussion Hernandez et al., 1996).

Second, if nonlinear character of rsEEG rhythms derive from the Takens' theorem, another preliminary run should test if the dynamics of the system and the mentioned observations are autonomous or reflect some other variables generated by another deterministic system. Based on the outcome, the nonlinear measurements will have to be adapted according to Stark et al. (2003).

Third, due to the lack of a pathophysiological model of deterministic nonlinear processes in brain disorders, the outcome of nonlinear analyses of rsEEG rhythms in clinical research should not be interpreted in terms of disease effects on deterministic chaos in the brain (see for an insightful discussion Pezard et al., 1994, and Pardey et al., 1996). Instead, a conservative descriptive approach should discuss the eventual correlation of nonlinear measures with relevant clinical features such as disease trait (i.e., the pathophysiology of the disease) or status (i.e., its progression or response to intervention). Furthermore, this characterization might be related to and correlated with qualified neuroimaging or fluid biomarkers of the disease to gain putative information on the pathophysiological relevance of nonlinear measures of rsEEG rhythms.

5.3. "Connectivity"

Resting state fMRI (rs-fMRI) unveiled separate brain networks formed by interdependent neural masses that underpin (1) the emotional coloring (i.e., salience), (2) planning, execution, and control of behavior (i.e., central executive), and (3) resting state condition (Damoiseaux et al., 2006). Their functional interdependence can be deranged in patients with initial stages of brain disorders (Damoiseaux et al., 2006; Chand et al., 2017).

In this theoretical context, *connectivity* is a key concept to describe the statistical interdependence between neural masses within and among those brain networks (Friston, 2011). The *functional* connectivity denotes the mutual information or statistical interdependence in the activity between two or more neural nodes

of a brain network, while the *effective*[8] connectivity designates either the temporal precedence or a causal influence in the activity of one neural node over another (Valdes-Sosa et al., 2011; Friston et al., 2013). A more conservative theoretical position states that in the framework of an experimental study, such an influence can be proved to be *causal* only under conditions that are changing due to an external intervention such as an experimental manipulation, a pharmacological treatment, a brain stimulation, etc. (Pearl, 2010). A general theory was proposed to test that hypothesis by a structural causal model (Pearl, 2010).

Functional and effective brain connectivity can be probed by fMRI, positron emission tomography (PET), EEG, magnetoencephalography (MEG), and intracranial EEG recordings, each with different spatial and temporal scales (for a review, see Sakkalis, 2011, and Damoiseaux and Greicius, 2009). EEG and MEG techniques have an ideal millisecond time resolution to investigate the role of brain oscillatory activity in that connectivity (Mantini et al., 2007; Stam and Reijneveld, 2007; D'Amelio and Rossini, 2012) and unveil neurophysiological mechanisms underlying sensorimotor, cognitive, and affective dysfunctions in patients with neurological and psychiatric disorders. Three main methodological approaches are reviewed in the following paragraphs.

A first approach estimates the interdependence of the phases of rsEEG rhythms at the electrode level (Kamiński and Blinowska, 1991; Baccalá and Sameshima, 2001; Blinowska, 2011; Fraschini et al., 2016; Stam, 2010; Stam and van Straaten, 2012). This approach was adopted by Brazier (1972) in a pioneering study aimed at estimating the individual spreading of spontaneous electrical seizure activity at given frequencies within the brain of epileptics during presurgical intracerebral EEG recordings. A basic assumption of this approach is that such interdependence at scalp electrode pairs may unveil the inter-relationship between the underlying cortical regions, without significant distortions due to

head volume conduction effects connected with the spread of source electric fields (Kaminski and Blinowska, 2017). Furthermore, some computational procedures of this approach can take into account the inflating effects of an "active" reference electrode on that interdependence (see the Section 5.3.1.). Overall, the advantage of this approach is that the phase of scalp rsEEG rhythms is not potentially distorted by source estimation procedures (Kaminski and Blinowska, 2017). Its disadvantage is that it ignores observational equations considering confounding effects of head volume conduction and position/orientation of cortical sources of scalp EEG activity (Schoffelen and Gross, 2009; Brunner et al., 2016; Van de Steen et al., 2016). Due to head volume conduction effects, electric fields can instantaneously spread from a brain source to several scalp electrodes, thus generating a spurious interdependence between scalp rsEEG activity recorded at those electrodes.

A second methodological approach adapts inverse solutions for the estimation of functional and effective source connectivity within spherical or realistic models of the head volume conductor and equivalent current dipoles as generator models (for a review, see Valdes-Sosa et al., 2011; Pascual-Marqui et al., 2011, 2014; Karahan et al., 2015). In the past years, there has been an improvement in the modeling of head volume conduction, EEG source estimation, and the measurement of source localization errors (Valdes-Sosa et al., 2011; Pascual-Marqui et al., 2011, 2014; Karahan et al., 2015). However, there is no unique solution to the inverse problem from the known scalp EEG activity to the estimation of cortical source activity. Indeed, inverse estimates of EEG cortical source activity and connectivity depend on forward and inverse models and several parameters, e.g. the anatomical head template and electrical source model, a-priori assumptions on source number, placement, and orientation, and weights for the lead field matrix linking scalp EEG activity and estimated source current density. Therefore, these techniques suffer from limitations in the biophysical modeling of head volume conduction and brain sources (e.g., modeling the influence of thalamocortical neurons on cortical pyramidal neurons). Furthermore, confidence limits of EEG source connectivity solutions are known just for a limited number of cases (Kaminski and Blinowska, 2017).

A good example of needed research for the second methodological approach is reported in a recent study (Mahjoory et al., 2017). The Authors of that study used scalp rsEEG data from two independent cohorts, two anatomical head templates (i.e., Colin27 and ICBM152), three electrical models (i.e., boundary element model, finite element model, and spherical harmonics expansions), three inverse methods (eLORETA, weighted minimum norm estimation, and linearly constrained minimum-variance beamformer), and three software platforms (Brainstorm, Fieldtrip, and a homemade toolbox). The main findings showed that inverse estimates of source activity were quite consistent across the above procedures. In contrast, different inverse estimation methods and software platforms induced a considerable variability in functional source connectivity. In this framework, eLORETA and weighted minimum norm estimation showed solutions more consistent with each other when compared to the beamformer results. As expected, these findings were more consistent within a given population cohort than between two cohorts.

A third methodological approach uses two basic methods. The first is based on spline or Hjorth Laplacian estimation of the radial current density inflowing or outflowing through the scalp from and to the cerebral cortex (Nunez and Srinivasan, 2006). The second computes the solution of the inner continuation inverse problem of the EEG, supplying the spatial distribution of the voltages on the dura mater model of the head volume conductor (Nunez and Srinivasan, 2006). Both Laplacian estimation and the solution of the inner continuation inverse problem use formal models of the

---

[8] Interesting procedures estimate the effective (directional) interdependence from rsEEG rhythms recorded at one scalp electrode to another, taking into account the reciprocal correlations of those rhythms between the scalp electrodes of an array. This directional relationship complements that indicated by the algorithms of functional brain connectivity for clinical research. The most used mathematical algorithms are based on Granger causality principle, multivariate autoregressive model and its variant for the analysis of rsEEG rhythms in the frequency domain, namely the directed transfer function (Blinowska and Kaminski, 2013). Furthermore, a procedure called "isolated effective connectivity" applied this concept to the estimation of effective connectivity of cortical sources of scalp EEG activity (Pascual-Marqui et al., 2014). When selecting a linear or nonlinear measure of functional or effective interdependence of rsEEG rhythms, several features of the estimator should be taken into account: robustness in respect of measurement or biological noise (blinking, saccades), sensitivity to "common drive" and "cascade flow" effects, and effects of head volume conduction (for more explanation, see the main text in the Section 5.3. Linear connectivity). Ideally, future research should compare the validity and reliability of different linear and nonlinear estimators of interdependence of rsEEG rhythms recorded at scalp electrodes and the application of those estimators in the modeling of functional and effective connectivity of their cortical sources. It can be speculated that a noticeable directionality of the connectivity from one electrode to another would suggest an effective or causal (i.e., hierarchical) relationship in the direction of the information flux from the former to the latter, although no straightforward interpretation can be made in terms of underlying cortical sources due to head volume conduction effects. Of note, directional interrelatedness might not always imply causal interrelatedness, e.g., directionality derived from the phase of coherence of rsEEG rhythms recorded at two scalp electrodes might not indicate causality of the interactions between the cortical neural populations generating those rhythms. Indeed, it is not entirely clear what is the specific neurophysiological meaning of that directionality. It might be related to (1) the conduction of action potentials between cortical and thalamic neural populations involved in the generation of rsEEG rhythms recorded at the pairs of scalp electrodes and/or (2) the modulation of synaptic potentials at those populations. To overcome the mentioned intrinsic limitations, techniques of effective connectivity have been implemented in the solution of the inverse problem to estimate EEG cortical sources (Valdes-Sosa et al. 2011; Pascual-Marqui et al., 2014). However, these techniques are model-dependent and do not provide a unique solution to the inverse problem. More research is needed to clarify the effect of the rsEEG source estimation on the accuracy of the reconstruction of that "directional flux."

head volume conductor to minimize the spread of electrical field from the cerebral cortex to the scalp surface (Babiloni et al., 2001). However, these methods may introduce inherent imprecisions in the estimated functional and effective cortical connectivity as the effects of the position and orientation of cortical sources in the head volume conduction are not explicitly modeled (Brunner et al., 2016; Van de Steen et al., 2016).

The above measures of interdependence of scalp rsEEG rhythms (scalp sensor level) or source connectivity (source level) can be used as inputs to procedures based on Graph theory,[9] which provides a metric for brain network analysis at the microscale, mesoscale, and macroscale (see D'Amelio and Rossini, 2012; Stam and Reijneveld, 2007). The Graph theory markers represent the configuration of network nodes and connectivity (e.g., nodes connecting many-few nodes in the same module), their modular configuration (e.g., nodes emanating many-few edges to nodes with high or low reciprocal interconnection), and the overall system topology, respectively (Medaglia, 2017). Among the outcome markers, a bulk of fMRI, rsEEG, and rsMEG studies has suggested that a small-world topology reflects system resiliency and effects of some brain disorders (Bassett and Bullmore, 2006; Stam and Reijneveld, 2007). However, this idea has been recently challenged (Blinowska and Kaminski, 2013). As with any relatively new methodological procedure, the application of the Graph theory to rsEEG rhythms needs caution and more clinical research before a final judgement. We recommend future experiments to define opportunities and limitations of this approach for Clinical Neurophysiology. Indeed, the topological Graph patterns depend on several potentially confounding variables: (1) the validity and reliability of the techniques used to estimate functional or effective connectivity of rsEEG rhythms (bivariate estimators may be prone to the common source effects potentially producing multiple false connections); (2) the statistical thresholds to qualify the significant associations between sensors or sources; and (3) the results of the measurement noise and intrinsic autocorrelation of rsEEG signals at scalp electrodes (Papo et al., 2016; Blinowska and Kaminski, 2013; Hlinka et al., 2017).

5.3.1. Linear measures of "connectivity"

Historically, the most used linear measurement of the functional interdependence of scalp rsEEG rhythms is the bivariate analysis of FFT-based spectral coherence[10] between single pairs of electrodes. In this context, bivariate means that at a given frequency, the estimation of the coherence of rsEEG activity at a single pair of electrodes does not consider the coherence values computed between other electrode pairs (In contrast, multivariate techniques provide that estimation considering that interdependence between all electrode pairs of the array). This bivariate measure of spectral coherence is defined as a correlation coefficient (squared) that esti-

mates the consistency of *relative amplitude and phase* between any pair of oscillatory signals in each frequency band (Nunez and Srinivasan, 2006). Unfortunately, spectral coherence and other (especially bivariate) measures of interdependence of rsEEG rhythms between scalp electrodes may be confounded by effects of *reference electrode, head volume conduction, common drive, and cascade flow* (Blinowska, 2011).

Reference electrode effect is well-known. If a given cortical rsEEG source is particularly active underneath the reference electrode site, the phases and frequencies of that activity are reflected in the rsEEG activity recorded at all exploring electrodes, inflating the spectral coherence and other (especially bivariate) measures of that interdependence computed between all scalp electrode pairs.

Head volume conduction effect is due to the instantaneous (i.e., no time lag) spread of electric fields generated by brain sources across cerebral cortex, cerebrospinal fluid, skull, and scalp. This effect can inflate the spectral coherence and other (especially bivariate) measures of interdependence of scalp rsEEG rhythms. Fig. 1 (upper row) shows some paradigmatic cases of the effect of head volume condition. In the figure, an ideal model of head volume conductor includes three exploring scalp electrodes (e.g., "a", "b", and "c") and four underlying cortical sources (e.g., "At", "ABr", "Br", and "Cr") whose spreading neural electric fields are associated with variations of scalp EEG activity. In the model, EEG activity (not shown) would be recorded with respect to a distant reference electrode (not shown). The source "At" is placed under the electrode "a" and has a tangential orientation to the scalp. The source "ABr" is placed between the electrodes "a" and "b" and has a radial orientation to the scalp. The source "Br" is placed under the electrodes "b" and has a radial orientation to the scalp. The source "Cr" is located under the electrode "c" and has a radial orientation to the scalp.

In the ideal model, the head volume conduction effect does not ever mix the spatial correspondence between cortical sources and scalp electrodes where EEG activity generated from those sources is recorded. For example (Fig. 1, upper row, left), the neural electric fields generated from the radial sources "Br" and "Cr" would spread to the overlying electrodes "b" and "c", respectively.

In other cases, the head volume conduction effect does mix the mentioned spatial correspondence. For example (Fig. 1, upper row, right), the neural electric fields generated from the source "At" would spread to the distant electrode "b" but not to the overlying electrode "a". Unfortunately, this misleading effect of the head volume conduction may not be removed by the Laplacian estimates of the scalp current density or the potential estimated at the dura mater level. As another example (Fig. 1, middle row, left), the neural electric fields generated from the source "ABr" would spread to both electrodes "a" and "b". Therefore, an activation of the source "ABr" would induce a significant coherence or other (especially bivariate) measures of interdependence of the rsEEG rhythms recorded at the electrodes "a" and "b", especially at the zero-lag component. A mistaken interpretation would explain that interdependence as due to a functional connectivity between the underlying cortical sources "At" and "ABr". Finally, let us consider a coherent activation of the sources "At" and "Cr" (Fig. 1, middle row, right). Neural electric fields of those sources would spread to the scalp electrodes "b" and "c", respectively. Of note, the electrode "b" does not overly the cortical source "At". This effect would determine a significant coherence or other (especially bivariate) measures of interdependence of the EEG activity recorded at these two exploring scalp electrodes, while the EEG activity recorded at the scalp electrodes "a" and "c" (overlying the sources "At" and "Cr") would show no significant coherence. A mistaken interpretation would explain that interdependence as due to a functional connectivity between the underlying cortical sources "Br" and "Cr".

---

[9] The significant contribution of Graph theory to the EEG field is the attempt to derive some general features of the brain connectivity in physiological and diseased conditions. The most used topological features of the Graph theory include the clustering coefficient, probing local neural network connectivity (C, pairs of near electrodes), and the individual interconnectional path length (L), defined as the length of the shortest paths connecting pairs of nodes as a measurement of the efficiency of the parallel information transmission within a given network. The Graph topology has been considered a promising variable to describe possible critical states of the brain dynamic systems during the transition between ordered and random behavior (this transition is supposed to have implications on information transfer, storage capacity, and sensitivity to external stimuli). It has been proposed that criticality of the brain dynamic system depends on phase synchronization and functional coupling of the oscillatory activity of neural populations as reflected by EEG and magnetoencephalographic (MEG) rhythms (Bassett et al., 2006). Overall, the actual studies on rsEEG "graphs" in neurological patients did not produce converging findings sufficiently mature for a systematic use in the clinical management of patients. Therefore, we will not get into more details in this paper.

[10] High coherence between the activity of two EEG brain sources means that their relationship reflects a linear transformation, although their underlying dynamics may be not necessarily linear (Srinivasan et al., 2007).

Keeping in mind those examples, the head volume conduction effect may confound the interpretation of measures of interdependence of rsEEG rhythms recorded at scalp electrodes in some cases. However, this effect generally decays with the distance between cortical sources and exploring scalp electrodes, although the curvature of the head and tangential orientation of the EEG sources may induce anti-correlated EEG activity and increased coherence at distant electrode pairs. A simulation study quantified this decay using a head conductor model based on three confocal ellipsoidal surfaces (i.e., scalp, skull, and cortex) with equivalent current dipoles as cortical source models (Srinivasan et al., 2007). Uncorrelated oscillatory activities were imposed in these dipoles, and EEG spectral coherence between virtual scalp electrode pairs was computed to measure the head volume conduction effect. Despite the incoherence of the dipole source activities, results showed a large spurious (false) EEG coherence between scalp electrodes separated less than approximately 10–12 cm (Srinivasan et al., 2007). Furthermore, there were mild spurious EEG coherence values even for distances between paired scalp electrodes greater than 20 cm, possibly due to head and source geometry (Srinivasan et al., 2007). Noteworthy, impact of head volume conduction effects on scalp EEG coherence may be magnified by the extension of underlying cortical EEG sources. In all frequency bands, EEG activity recorded at a given scalp electrode is estimated to reflect the mean over all synchronous cortical sources distributed in a vast cortical region of many squared centimeters (Nunez and Srinivasan, 2006).

Common drive effect denotes the physiological conduction (i.e., with some time lag) of action potentials through axons from a brain neural mass to two (or more) cortical neural masses (sources) generating neural electric fields recordable as EEG activities at scalp electrodes. This effect is illustrated in Fig. 1 (lower row, left). Let us consider the neural mass of the source "Cr" sending action potentials through neuronal axons to the sources "Br" and ABr" (where the "Br" and "ABr" sources have no functional connectivity between them). In the example, the action potentials would arrive before and be more effective at the source "Br" than the source "ABr". This sequential event would induce a significant non-zero lag interdependence of the rsEEG rhythms between electrodes "c" and "b", "c" and "a", and "b" and "a". An erroneous interpretation would explain that interdependence as due to a functional connectivity between the sources "Br" and "ABr" as well as between the sources "Cr" and "At". In the same line, bivariate inverse estimations of cortical source connectivity from scalp EEG activity may suggest a (spurious) functional cortical connectivity between "Br" and "ABr" sources. Overall, the common drive

effect may induce many spurious solutions of interdependence at scalp (source) level (Blinowska, 2011; Blinowska and Kaminski, 2013).

Cascade flow effect is also related to the physiological conduction (i.e., with some time lag) of action potentials through axons from a brain neural mass to another (or more) cortical neural masses acting as cortical sources of scalp EEG activity. An example of this effect is illustrated in Fig. 1 (lower row, right). Let us consider the following sequence of cortical source activations. Firstly, the neural mass of the source "Cr" sends action potentials through neuronal axons to the source "Br". When activated, the neural mass
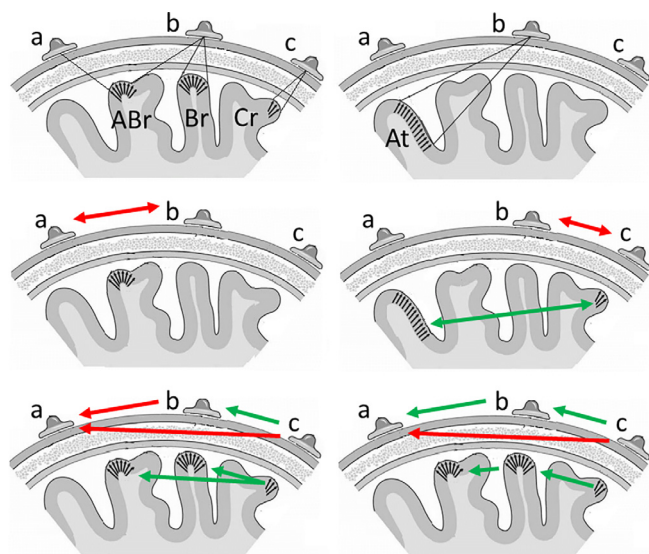

Fig. 1. Some examples of the effects of the head volume conduction, "common drive", and "cascade flow" (for an explanation, see the main text in Section 5.3.1. "Linear measures of connectivity") confounding the interpretation of the results of the techniques for the computation of functional and effective connectivity from rsEEG rhythms. UPPER ROW. Some examples based on a model with three exploring scalp electrodes "a", "b", and "c" and four underlying cortical sources "At" (i.e., under the electrode "a" with a tangential orientation), "ABr" (i.e., halfway between the electrodes "a" and "b" with a radial orientation), "Br" (i.e., under the electrode "b" with a radial orientation), and "Cr" (i.e., under the electrode "c" with a radial orientation). In the model, the source "At" electric fields are volume conducted to the electrode "a". The source "ABr" electric fields are volume conducted to the electrodes "a" and "b". The source "Br" electric fields are volume conducted to the electrode "b". The source "Cr" electric fields are volume conducted to the electrode "c". In this model, the electrode "b" records electric fields generated by both the cortical tangential source "At" and the cortical radial sources "ABr" and "Br". Due to effects of cortical source localization/orientation and head as a volume conductor, phase and amplitude of EEG signals collected at a given exploring scalp electrode would reflect a weighted average of contributions of cortical sources in relation to their respective distance from that electrode. Indeed, electric fields generated from a cortical source decay to zero values at 10–12 centimeters of distance, with possible additional mild effects for distances greater than 20 cm due to head and source geometry (Srinivasan et al., 2007). Noteworthy, the impact of head volume conduction effects is magnified by the extension of underlying cortical EEG sources. In all frequency bands, EEG activity recorded at a given scalp electrode may reflect synchronous cortical sources distributed in a vast cortical region of tens of squared centimeters (Nunez and Srinivasan, 2006). In the ideal model of the figure, the possible synchronizing influence of thalamocortical neural populations is not shown. Furthermore, EEG activity (not shown) at exploring scalp electrodes "a", "b", and "c" would be recorded relative to a distant reference electrode (not shown). MIDDLE ROW, LEFT. Due to the effect of head volume conduction, an activation of the source "ABr" may induce an interdependence of rsEEG rhythms recorded at the electrodes "a" and "b". Such interdependence could be erroneously interpreted as a functional connectivity between the cortical sources "At" and "Br", underlying those electrodes. MIDDLE ROW, RIGHT. Due to the effect of head volume conduction, a coherent activation of the sources "At" and "Cr" may induce an interdependence of the rsEEG rhythms recorded at the electrodes "b" and "c". Such interdependence could be erroneously interpreted as a functional connectivity between the cortical sources "Br" and "Cr", underlying those electrodes. LOWER ROW, LEFT. Due to the effect of "common drive", a coherent activation of the source "Cr" with the sources "Br" and ABr may induce an interdependence of the rsEEG rhythms recorded at the electrodes "a" and "c" and those recorded at the electrodes "b" and "a". Such interdependence could be erroneously interpreted as a functional connectivity between the cortical sources "At" and "Cr" and between the cortical sources "Br" and "ABr", underlying those electrodes. LOWER ROW, RIGHT. A directional connectivity from the source "Cr" to "Br" and from "Br" to "ABr" is illustrated to show the difference between "direct" and "indirect" connection pathways. In the figure, there is a "direct" connection pathway from the source "Cr" to the source "Br", while the connection pathway is "indirect" between the sources "Cr" and "At". In the figure, the source "Br" also shows a directional connectivity to the source "ABr". Due to the effect of "cascade flow", this pattern of source connectivity may induce a directional interdependence of the rsEEG rhythms recorded at the electrodes "c" and "a". Two erroneous interpretations of that interdependence at the scalp sensors would infer a functional connectivity between the sources "Br" and "ABr" as well as between the sources "Cr" and "At". In the figure, the green arrows between the scalp electrodes indicate the interdependence of EEG activity (not shown) at the sensor level that would correspond to the functional connectivity between the underlying cortical sources, indicated by green arrows as well. In this case, such interdependence unveils the true underlying functional cortical connectivity. In contrast, the red arrows between the scalp electrodes indicate the interdependence of EEG activity (not shown) at the scalp level that would not correspond to the functional connectivity between the underlying cortical sources, indicated by red arrows as well. In this case, such interdependence provides a misleading representation of the underlying functional cortical connectivity.

of the source Br sends action potentials through neuronal axons to the source "ABr" (where the sources "Cr" and "ABr" have no functional connectivity between them). This example illustrates the difference between "direct" and "indirect" connection pathways. There is a "direct" directional connection pathway from the source "Cr" to the source "Br", while the connection pathway is indirect from the source "Cr" to the source "ABr". This sequence of source activations would induce the following directional interdependence of the scalp rsEEG activity: (1) from the electrode "c" to the electrodes "b" and "a" and (2) from the electrode "b" to the electrode "a". A mistaken interpretation would explain that directional interdependence as due to an effective connectivity from the source "Cr" to the source "At".

Frontal positive and parietal negative P20/N20 peaks of somatosensory evoked potentials following the electrical stimulation of right median nerve at the wrist is an interesting example of the remarkable effects of human head volume conduction in the case of an activation of a physiological cortical generator oriented tangentially to the scalp surface. These peaks are generated at about 20 milliseconds post-stimulus in the primary somatosensory cortex, buried in the Rolandic central sulcus (i.e., postcentral Brodmann area 3b). However, the maximum amplitude of these peaks at the scalp is observed in anterior and posterior regions far from the central sulcus (Seiss et al., 2002). It can be speculated that when similar precentral, central, and postcentral tangential sources show a fluctuating activation during a resting state condition, estimates of an intrahemispheric functional connectivity from rsEEG rhythms between pairs of scalp electrodes or estimated cortical sources might be inflated. Indeed, the influence of those physiological tangential cortical sources in the resting state condition might be relatively one-third lower when compared to cortical radial sources (Srinivasan et al., 2007). However, more research is needed to weight the effects of head volume conduction on results of functional/effective connectivity and source estimation techniques applied on rsEEG rhythms.

Keeping in mind the above considerations and examples, our recommendations for future research are reported in the following.

First, the computation of interdependence of rsEEG rhythms between scalp electrodes or inverse estimates of source connectivity can be improved by methods estimating lagged components of that interdependence or source connectivity. These methods include bivariate and multivariate techniques. Input EEG variables for bivariate techniques refer to two paired (scalp) electrodes or (cortical) sources, while those for multivariate techniques refer to multiple electrodes or sources.

Bivariate techniques include the computation of imaginary part of coherency between rsEEG rhythms at electrode or source pairs, this part being zero with uncorrelated cortical source activity (Nolte et al., 2004). Phase lag index estimates the interrelatedness between rsEEG rhythms with lagged phase synchronization at electrode pairs (Stam et al., 2007, 2010). Linear lagged connectivity estimates linear inverse source connectivity as lagged phase synchronization (Pascual-Marqui et al., 2011).

Multivariate methods based on Granger causality principle and autoregressive (MVAR) model are the most used for application to rsEEG data and are grounded on covariance matrices at different lags of phase synchronization for all electrodes or sources of interest. This approach assumes that causes temporally precede their effects in a predictable way (Granger, 1969), and computational procedures can account for the common-drive phase synchronization of EEG rhythms mentioned above (Kamiński and Blinowska, 1991). Of note, this general multivariate approach can be applied to compute the interdependence of EEG activity recorded between electrodes placed at the scalp, cortical or sub-cortical level as well as for the estimation of functional connectivity between brain source activities modeled solving the EEG inverse problem. In line

with the article aim, here we will focus on its application on scalp rsEEG potentials and estimated cortical source activities.

For the first time, the following procedures were derived from methods based on Granger causality principle and MVAR model to estimate the interdependence of EEG activity recorded from scalp electrodes. Under assumptions of stationary EEG epochs and linear processes, Directed Transfer Function (DTF) solutions were used to estimate directional lagged phase synchronization in EEG rhythms between scalp electrodes (e.g., "a" to "b" and "b" to "a" scalp electrodes) by a procedure modeling the potential effects of common-drive phase synchronizations of EEG rhythms recorded at the other scalp electrodes of the array (Kamiński and Blinowska, 1991). Under the same assumptions, partial directed coherence (PDC) solutions were used to estimate "direct" lagged phase synchronizations in EEG rhythms between two scalp electrodes, taking into account "cascade-flow" phase synchronization of EEG rhythms recorded at the other scalp electrodes of the array. Theoretically, PDC solutions are not misled by indirect lagged phase synchronizations of EEG rhythms between scalp electrodes (e.g., "a" – "b" and "b" – "c" but not "a" – "c" scalp electrodes; Baccalá and Sameshima, 2001).

More recently, the following advanced versions of above procedures were proposed: (1) renormalized PDC (rPDC), for renormalizing PDC solutions taking into account the number of *receiver electrodes* (Schelter et al., 2009) and (2) direct DTF (dDTF), for being not affected by indirect lagged phase synchronizations of EEG rhythms between scalp electrodes, similarly to PDC pros (for a review see Blinowska, 2011). Furthermore, a procedure called isolated effective coherence (iCoh) was proposed to provide measures related to PDC under a MVAR model at (eLORETA) cortical EEG source level, followed by zeroing all irrelevant associations to zero to focus on directional associations of interest at that source level (Pascual-Marqui et al., 2014).

The mentioned multivariate methods are more advantageous than bivariate ones, since they reduce the spurious interdependencies of rsEEG rhythms at the scalp or source level due to common drive and cascade flow effects. In estimation of parameters of the MVAR model, the following issues have to be considered: (1) adequate model order and EEG epoch length should be chosen; (2) the issue of signal stationarity across EEG epochs should be properly taken into account (Pereda et al., 2005); (3) all major driving forces of rsEEG rhythms have to be represented in that model (Blinowska and Zygierewicz, 2012; Blinowska and Kaminski, 2013; Pascual-Marqui et al., 2014). For example, there may be an underrepresentation of the common sources localized in sensorimotor thalamocortical populations targeting cortical pyramidal neurons that contribute to the generation of scalp rsEEG rhythms.

Second, neurophysiological inferences from results of the above multivariate methods should be considered with caution, although their solutions are more helpful than the bivariate ones. On one hand, it has been stated that multivariate approaches grounded on Granger causality and MVAR models can provide insights in clinical research based on DTF and PDC solutions computed from scalp rsEEG signals (Kuś et al., 2004; Blinowska and Kaminski, 2013). For example, compared with healthy control subjects, Alzheimer's disease patients with dementia were characterized by decreased strengths of non-normalized DTF solutions, especially at posterior electrodes, and lower rate of their decay as a function of scalp inter-electrode distance (Blinowska et al., 2017). These variables were clinically relevant as the combination of those DTF solutions, MVAR-based spectral coherence, and feature extraction procedures (e.g., principal component analysis and computation of Mahalanobis distance) resulted in a classification accuracy of 86% (area under the receiver operating characteristic) in the discrimination of individual control subjects and patients (Blinowska et al., 2017). On the other hand, it should be remarked that those interdependence measures

at the scalp level may not reflect the true connectivity between the underlying cortical neural masses, due to the lack of biophysical models of head volume conduction and sources (Brunner et al., 2016; Van de Steen et al., 2016). In other words, under the mentioned assumptions, the family of DTF and PDC solutions reduce spurious interdependencies at the scalp level due to common drive and cascade flow (Blinowska and Zygierewicz, 2012). However, this advantage does not ensure that the resulting pattern of interdependence reflects the underlying pattern of source cortical connectivity (Brunner et al., 2016; Van de Steen et al., 2016). More research is needed to clarify this issue.

Third, in ideal simulation studies, scalp and cortical rsEEG rhythms might be mathematically-generated by different combinations of equivalent current dipoles distributed in cortical and subcortical compartments of a realistic head volume conductor constructed using MRI. These combinations may include paradigmatic cases of coherent and incoherent activations of dipoles with different signal-to-noise ratio and experimental manipulations producing common drive and cascade flow effects. Solutions of different "connectivity" techniques may be compared to define their pros and cons in the various experimental manipulations. Among promising in-vivo studies, different "connectivity" techniques may be applied to rsEEG data obtained by recordings from scalp (a day before the implantation of intracranial EEG electrodes) and intracranial electrodes (a day after that implantation) in epilepsy patients resistant to pharmacological treatment. The comparison of the interdependence pattern of scalp rsEEG activity vs inverse estimates of cortical source connectivity may be invaluable to clarify pros and cons of those "connectivity" techniques comparatively.

Fourth, another ideal in-vivo approach for the study of the head volume conduction, common drive, and cascade flow effects on EEG activity might be based on the transcranial magnetic stimulation (TMS) of cortical sites and the simultaneous scalp EEG recording (Bergmann et al., 2016; Ziemann, 2011). Indeed, the TMS over a cortical site is a casual intervention that induces an unequivocal effective connectivity from that site to other cortical sites producing evoked potentials (Rogasch and Fitzgerald, 2013) and, for example, changes in ongoing alpha rhythms (Capotosto et al., 2009, 2014). This effective connectivity can also be modulated by enhanced cortical inhibition due to either paired-pulse TMS with interstimulus intervals of 50–200 ms (Rogasch and Fitzgerald, 2013) or the administration of GABAergic receptor modulators (Darmani et al., 2016; Premoli et al., 2014). However, it should be remarked that TMS can induce not only neurotransmission from the stimulated cortical site but also electromagnetic artifacts confounding the interpretation of EEG readouts (Bergmann et al., 2016; Ziemann, 2011). Therefore, special attention must be devoted to the removal of these artifacts by an accurate preliminary analysis (Rogasch and Fitzgerald, 2013).

Fifth, emerging techniques of frequency analysis of the rsEEG rhythms explore the linear relationships between the phase of a given frequency and the amplitude of another related frequency.[11]

---

[11] An emerging branch of the functional brain "connectivity" from rsEEG rhythms is represented by the so-called phase-amplitude cross-frequency coupling (CFC). Phase-amplitude CFC at a given electrode pair or rsEEG source pair does model the dependence between the phase of a low-frequency (e.g., delta or theta) rsEEG coupling and the amplitude of that coupling at higher (e.g., beta or gamma) rsEEG frequencies (Canolty et al., 2006; Demiralp et al., 2007; Osipova et al., 2008; Cohen et al., 2009) even in some clinical applications in movement disorders (Miocinovic et al., 2015; Cole et al., 2017). However, the CFC analysis and the corresponding interpretation from a physiological point of view should consider some problems. For instance, some spectral CFC correlations can be merely due to common nonstationarities and nonsinusoidal features of the neural oscillations. These phenomena can arise even in the absence of true interactions between neural populations oscillating at given frequencies. Some solutions and procedural recommendations have been proposed to tackle these spurious CFC correlations and make more reliable the results of the CFC analysis (Aru et al., 2015; Jensen et al., 2016).

They require further investigations about reliability and robustness to signal-to-noise in the EEG data before the use in clinical research.

5.3.2. Nonlinear EEG time series models and measures of "connectivity"

Time series of two coupled nonlinear oscillators may display phase synchronization even when the amplitude of the relative oscillations is uncorrelated over time (Rosenblum et al., 1996). This fact suggests that if two brain neuronal populations show oscillatory nonlinear dynamics and reciprocal interaction, linear measures of their EEG activity such as spectral coherence could not detect that interaction with accuracy. To overcome this limitation, Information theory can be used to account for specific nonlinear features of interdependence of rsEEG rhythms at scalp electrodes or inverse estimates of cortical source connectivity (Jeong et al., 2001a,b; Schlögl et al., 2002; Na et al., 2002; Huang et al., 2003; Pascual-Marqui et al., 2011). The mutual information between the measures of rsEEG rhythms at the electrodes or sources X and Y can be estimated as the amount of information that the measured time series X provides about Y and vice-versa (Mars et al., 1985). Another index of interest is the cross-prediction, which measures the extent to which prediction of X is improved by knowledge about Y as a *directional* information about the nonlinear interdependence between X and Y.

Based on the above theoretical premises, several nonlinear procedures have been developed and applied to study functional and directional interdependence of rsEEG rhythms at scalp electrodes (for reviews, see Jeong, 2004; Pereda et al., 2005; Stam, 2005; Sakkalis, 2011; Dauwels et al., 2010). They include phase synchronization, general synchronization, synchronization likelihood, state-space based synchrony, stochastic events synchronization, the synchronization likelihood, mutual information, permutation conditional mutual information, and nonlinear interdependence (Jeong et al., 2001a,b; Pereda et al., 2005; Dauwels et al., 2010; Wen et al., 2015).

Compared to the broad concept of "synchronization" defined in a previous section, those techniques use it with the notion that two or many brain areas or regions adjust some of the time-varying properties of their activity to a common behavior due to coupling or common external forcing. Among several indexes with these properties, phase synchronization is suitable to detect nonlinear dynamics in the interdependence between two rsEEG time series when they are characterized by a non-uniform distribution of their phase difference. Furthermore, generalized synchronization can be used when the two rsEEG time series X and Y are expected to reflect two interacting brain systems where the state of the first system depends on that of the second one (Jansen et al., 2003; Le Van Quyen et al., 1998; Breakspear and Terry, 2002).

We remark that the same concerns and limitations in the analysis of linear interdependence of two rsEEG time series apply to the nonlinear analysis. For example, nonlinear estimates enumerated above are bivariate, so they markedly suffer from the *common drive* effect. When applied to rsEEG signals recorded from scalp electrodes, their solutions are also influenced by the head volume conduction effect. When applied at source level, they suffer from the lack of a unique solution to the EEG inverse problem as well as limitations in the biophysical modeling of head volume conduction and brain sources. Furthermore, other challenging issues are the identification of best parameters and rsEEG epoch length as well as the issue of signal stationarity across rsEEG epochs, except for methods based on matching pursuit (Durka et al., 2005; Pereda et al., 2005; Dauwels et al., 2010). Moreover, the performance of nonlinear methods such as mutual information and phase-based estimators may be affected by levels of noise that can be seen in rsEEG data (>5%; Netoff et al., 2006). Finally, a practical methodological aspect is that the set-up of those nonlinear procedures

needs adequate expertise and computational resources when compared to the standard spectral analysis of rsEEG data by linear procedures (e.g., spectral coherence, etc.). The above issues should be carefully considered in the application of nonlinear rsEEG features for clinical research.

A main scientific question is the specific and comparative value of linear and nonlinear measurements of interdependence of rsEEG rhythms or inverse estimates of cortical source connectivity. To date, systematic comparisons of these measurements are scarce, and findings cannot be considered as conclusive. Some relevant findings are summarized in the following.

First, a comprehensive review of the literature reported that nonlinear (e.g., generalized synchronization, phase synchronization, and event synchronization) and linear methods estimating interrelatedness of rsEEG activity produce indexes basically correlated with each other (Pereda et al., 2005). Furthermore, generalized synchronization, nonlinear Granger causality, and the information-theoretic solutions may be preferable for investigating nonlinear interdependence considering amplitudes of rsEEG rhythms, while phase synchronization may be preferable when this is not the case (Pereda et al., 2005). The Authors of that review (Pereda et al., 2005) concluded that the linear approaches should be the first choice, going to the more complicated nonlinear ones when there is an evidence of nonlinearity (surrogate data as control reference).

Second, in a comparative clinical study (Dauwels et al., 2010), linear and nonlinear measures of interdependence of rsEEG rhythms derived from the correlation coefficient, mean-square and phase coherence, Granger causality principle (e.g., PDC, DTF, dDTF, full-frequency DTF), phase synchrony indices, information-theoretic divergence, state space based indices, and stochastic event synchrony were applied on data recorded in elderly patients with mild cognitive impairment (MCI) and age-matched control (Nold) subjects. As a result, the only measures weakly correlated with the coefficient of correlation were those derived from phase synchrony indices, Granger causality, and stochastic event synchrony. Therefore, it was concluded that each of them might reveal an aspect of the interdependence between pairs of rsEEG time series at the scalp level. Concerning the clinical validation of those indices (Dauwels et al., 2010), only two could significantly discriminate MCI patients from the controls, namely stochastic event synchrony[12] (SES) and full-frequency DTF. On one hand, SES quantifies the similarity between point processes (of a countable subset) from the time-frequency representations of rsEEG rhythms obtained at a pair of two electrodes (sources). The procedure for the SES computation can be applied at rsEEG rhythms generated by any kind of brain process, namely deterministic-random, linear-nonlinear, stationary-nonstationary, etc. (For this reason, it belongs to methods for the analysis of nonlinear processes underlying EEG rhythms; Pereda et al., 2005). On the other hand, ff-DTF is a measure derived from linear Granger causality (for a review, see Blinowska and Zygierewicz, 2012). Results showed that the SES reached 68% and 75% of classification accuracy in the discrimination of Nold and MCI individuals as measured by linear and quadratic discriminant analyses, respectively. Instead, the ff-DTF reached 70% by both linear and quadratic discriminant analyses. When those two measures were combined, the classification accuracy reached 83% by both linear and quadratic discriminant analyses. These findings were confirmed by another

study of the same research group (Dauwels et al., 2010), the two studies being good research models for future comparisons of linear and nonlinear measures.

Third, in another mentioned study (Wendling et al., 2009), linear and nonlinear regression, phase synchronization, and generalized synchronization methods of interdependence of EEG activity were applied on *virtual* data mathematically generated to produce three classes of functional interdependence: (1) coupled stochastic signals; (2) coupled nonlinear dynamical systems (e.g., Rössler-Rössler and Hénon-Hénon coupled systems); and (3) coupled neuronal populations by a physiologically-relevant computational model. In each class, properties of paired *virtual* EEG signals included (1) a coupling from 0 (independent signals) to 1 (identical signals) as phase or amplitude relationship; (2) narrow vs broad frequency band; and (3) added noise 0% and 50% to signal on connectivity measures. Findings indicated that (1) some methods were insensitive to the imposed coupling parameter; (2) performance of those methods was dependent on the extension of the frequency band; and (3) there was no *ideal* method, namely none of the methods performed better than the other ones in all studied situations and evaluation criteria (e.g., mean square error, mean variance, and local relative sensitivity; Wendling et al., 2009).

Keeping in mind the above considerations, we recommend that future investigations compare linear and nonlinear measures of interdependence of rsEEG rhythms at scalp electrodes and inverse estimates of cortical source connectivity in healthy and neurological subjects. Furthermore, this comparison may be performed on data generated by physiologically-relevant computational models as a basis of future consensus statements guiding an application of nonlinear rsEEG connectivity estimates in clinical practice.

5.3.3. The steps of "connectivity" analysis

In general, the computation of interdependence of rsEEG rhythms at scalp electrodes and inverse estimates of cortical source connectivity allows the visualization of absolute or normalized magnitude values of those indices, frequency-bin-by-frequency-bin (i.e., the normalized values across all frequencies of interest, typically ranging from 0 to 1), for electrode pairs of interest or pairs of rsEEG cortical sources (*vide infra*). This computation is performed for the extraction of quantitative markers from delta to gamma frequency bands. The extracted indices probe physiological and pathological mechanisms of coupling/interdependence of the cortical neural synchronization for the regulation of vigilance in the resting state condition. Specifically, rsEEG connectivity is typically tested for intra-hemispherical frontoparietal regions and inter-hemispherical frontal, parietal, and temporal regions. The same frequency bands of the rsEEG amplitude/power density analysis (e.g., delta, theta, alpha, and several beta and gamma bands) are used. It should be remarked that this approach is mostly used in an exploratory context of clinical research, and consensus on its physiological interpretation and standardized use still is to be determined.

In a similar vein, to date, there is insufficient standardization of some steps of the analysis, namely the length and number of the rsEEG epochs to be used for the different linear or nonlinear indices of interdependence of rsEEG rhythms at scalp electrodes and inverse estimates of cortical source connectivity. Furthermore, there is no clear consensus on the statistical thresholds for the confirmation of a significant effect at the scalp or source level. Moreover, there is no consensus yet on the best-validated markers for clinical research, even if the most frequently-used measurement is the computation of the lagged part of linear spectral coherence of rsEEG rhythms between scalp electrode pairs. We recommend that future studies will clarify the above procedural points.

---

[12] With stochastic event synchrony (SES), the time-frequency transform at each electrode is approximated as a sequence of "bumps" in the time-frequency readout. At one electrode, each "bump" is considered as an "event" and reflects a prominent EEG oscillation in narrow frequencies during a brief period in the EEG epoch analyzed (Dauwels et al., 2010). SES is an index of the degree of "synchrony" between the "bumps" at the two paired electrodes. The higher that "synchrony", the higher the linear or nonlinear interdependence between the rsEEG rhythms at the paired electrodes.

6. Topographic analysis of scalp rsEEG rhythms

Topographical mapping of the rsEEG rhythms may be considered as part of the *statistical parametric mapping*, which is based on two general statistical frameworks such as *change distribution analysis* and *significance probability mapping* (Friston et al., 1994). In this frame, the *significance probability mapping* was developed in the analysis of multichannel EEG data and the construction of interpolated pseudomaps of a statistical parameter (Friston et al., 1994).

Here we arbitrarily considered three broad classes of topographical procedures to be applied to scalp rsEEG rhythms: (1) the *scalp topographic mapping*, which refers to the spatial distribution of frequency features over the scalp; (2) the *cortical source mapping*, which denotes the estimates of neural currents in source models located within a model of the head volume conductor; (3) the *surface Laplacian* and the solution of the *inner continuation problem*, which provide estimates of current density at the scalp electrodes and dura surface potential distribution, respectively (Nunez and Srinivasan, 2006). These analyses are performed frequency-bin-by-frequency-bin or for frequency bands of interest from delta to gamma. The three classes of procedures can probe pathophysiological mechanisms of cortical neural synchronization for the regulation of brain arousal and vigilance in the resting state condition.

6.1. Topographic mapping

Topographic mapping allows the visualization of the spatial distribution of the absolute or normalized rsEEG amplitude/power density or other linear or nonlinear measures of local cortical neural synchronization. Topographic mapping algorithms are variable, employing a linear, quadratic or spline interpolation of the rsEEG variables in the spatial samples (electrodes or sources). Since there is no consensus about the best interpolation procedure, we suggest using a few interpolation techniques for cross-validation purposes. Furthermore, any inference of the underlying cortical source activity should be considered with caution for the head volume conduction effects.

Although the isopotential lines in instantaneous maps of the EEG potential distribution are invariant to the choice of reference electrode (see Michel et al., 2004), the EEG time course and thereby the spectral estimates of the rsEEG rhythms created with single electrode references placed at scalp sites (i.e., cephalic references) have the risk of being substantially distorted ('scalloping') near the scalp reference site. This distortion problem can be partially avoided by using spatial average references or the computation of rsEEG scalp current density estimates (e.g., surface Laplacian operator; Perrin et al., 1987, Hjorth, 1991). When spline interpolation is used, results at border electrodes should not be used for possible computation artifacts.

When research hypotheses target scalp voltage (but not scalp current density) distributions of rsEEG rhythms, the average reference across all exploring electrodes and the computation of the *infinite reference* provide valid solutions. For a practical computation of the infinite reference, a procedure called *reference electrode standardization technique* (REST) is available in the literature (Yao, 2001; Yao et al., 2007) and has been validated by independent groups (Chella et al., 2016; Lei and Liao, 2017).

6.2. Cortical source mapping

Compared with scalp rsEEG topographic mapping, rsEEG source estimation allows disentangling the respective contribution of different cortical generators of scalp rsEEG rhythms (Babiloni et al., 2015).

Several linear and nonlinear mathematical procedures can be used for the estimation of the activity (i.e., neural current density) in cortical sources of the rsEEG rhythms (Valdés-Sosa et al., 2009; Gramfort et al., 2013). The techniques typically estimate an inverse solution with the minimum norm, weighted resolution optimization or weighted minimum norm solution (Pascual-Marqui et al., 2002, 2007; Phillips et al., 2002; Yao and He, 2001). They typically model 3D tomographic neuroimages of distributed rsEEG cortical generators. The estimates of the inverse solutions approximate the neural current density into a spherical or an MRI realistically-shaped head model formed by compartments representing the electrical properties of the scalp, skull, and cerebral cortex. The compartment for the cerebral cortex is usually co-registered to statistical parametric mapping (SPM) software coordinates or the Talairach brain atlas (Talairach and Tournoux, 1988).

In tomographic methods, the brain compartment of the head model is formed by hundreds to thousands of voxels with a variable (mm) spatial resolution. Any voxel contains an equivalent current dipole, fixed as position and orientation. Solutions estimate the current intensity of all equivalent current dipoles of the cerebral cortex to explain the scalp rsEEG amplitude/power density. Noteworthy, solutions of the EEG inverse problem are underdetermined and ill-conditioned, when the number of spatial samples (e.g., scalp electrodes) is lower than that of the unknown samples (e.g., equivalent current dipole used). For this reason, these solutions are mathematically regularized to estimate the best rsEEG cortical source solution. Essentially, the feature of the regularization procedures is one of the main aspects that distinguish the different techniques for the rsEEG cortical source estimation[13]. As the use of different regularization techniques returns different source solutions starting from the same scalp EEG topography, it follows that there is no unique solution to the EEG inverse problem. This limitation should be considered in the interpretation of findings of clinical research.

To reduce the natural variance across the individuals of a given population, the estimated rsEEG source activity is normalized per subject. A typical procedure consists in scaling any estimated dipole current density at each voxel and frequency bin by the mean or the sum of the dipole current density computed across all frequencies of interest (e.g., 0.5–45 Hz) and voxels of the brain volume. This procedure of normalization typically fits rsEEG variables into a Gaussian distribution and reduces inter-subject variability (Leuchter et al., 1993). After this normalization, rsEEG source solutions lose the original physical dimension and are represented by *normalized units*. In this scale, the value "1" is equal to the mean or the sum of the dipole current density at all frequencies (e.g., 0.5–45 Hz) and voxels of the brain volume.

For the analysis of rsEEG sources, the above techniques are more often applied than an alternative historical approach changing the location and orientation of one or few single equivalent current dipoles until the best fit of the scalp distribution of the rsEEG amplitude/power density is reached (Mosher et al., 1999). In this approach, the a priori knowledge on the number and position of those sources can inspire the procedure to derive the time evolution of estimated cortical activity.

---

[13] There are diverse ways to measure the quality of the solutions of the inverse problem of the EEG. Three usual solutions are EEG source localization error, full width at half-maximum (FWHM), and visibility (i.e., the ratio of the reconstructed to actual source amplitude). The FWHM is affected by the number of electrodes as well as the amount of regularization. The simulation studies should use all of them. Interesting examples of proper simulation studies used normative databases (Bosch-Bayard et al., 2001) and tested the presence of signal at each voxel of the EEG source space of the head model (Pascual-Marqui et al., 2002; Pascual-Marqui, 2007).

6.3. Estimation of scalp current density and dura surface potential

The estimation of scalp current density and dura surface potential estimation is often performed by spline-Laplacian algorithms and the solution of the inner continuation problem, respectively (Perrin et al., 1987, 1989; Pascual-Marqui et al., 1988a,b; Nunez, 1989, 2010, 2012; Babiloni et al 2001; Nunez and Srinivasan, 2006; Kayser and Tenke, 2015). Less often, Laplacian estimation is computed using the Hjorth's procedure (Hjorth, 1991).

The scalp spline-Laplacian and the solution of the inner continuation problem act as a sort of band pass spatial filter with peak sensitivity to 3–6 cm scale synchronous cortical source regions (a very approximate diameter), while unprocessed potentials are most sensitive to roughly the 5–15 cm scale (Nunez and Srinivasan, 2006). The advantages of these techniques are (1) full independence of the choice of reference electrode site and (2) independence of assumptions about the unknown sources, e.g., isolated dipoles. Compared with the solution of the inner continuation problem, the scalp spline-Laplacian is based on a quite simple model of the head volume conductor (Nunez and Srinivasan, 2006). Good spline Laplacian estimates need dense scalp electrode arrays (i.e., ≥48–64 electrodes) and low to moderate noise (depending on applications) in the rsEEG data (Nunez and Srinivasan, 2006; Bosch-Bayard et al., 2012). To mitigate noise influences, we recommend that Laplacian estimation is performed and averaged across 200 or more contiguous spatial samples (i.e., instantaneous) potential distributions).

6.4. Mapping cortical "connectivity"

As mentioned in an earlier section, the activity at any rsEEG source is often related to instantaneous (zero-lag) voltage changes at all scalp electrodes. Furthermore, the estimation of the instantaneous coherence between two cortical rsEEG sources might also be affected by another rsEEG source (i.e., the *common drive* effect). Therefore, a conservative approach to functional connectivity estimates is to compute the lagged part of EEG coherence between sources (Pascual-Marqui et al., 2011, 2014). That said, many data, especially in the alpha band, show cases where coherence falls off with moderate electrode separation (10–12 cm; Srinivasan et al., 2007) but then rises to near zero-lag levels at large (>10 cm) distances. Furthermore, Laplacian-based coherence can be moderate to large at big distances, and these might not be due to reference or volume conduction effects (Nunez and Srinivasan, 2006). Therefore, future basic research should provide new insights about how to manage the zero-lag coherence solutions in the analysis of functional interdependence of rsEEG rhythms. An ideal multimodal approach may compare functional interdependence of rsEEG rhythms at scalp electrodes, inverse estimates of cortical source connectivity, the solution of the inner continuation problem, the scalp spline-Laplacian distribution, and raw EEG data (Nunez and Srinivasan, 2006; Pascual-Marqui et al., 2011; Blinowska and Zygierewicz, 2012).

The spatial resolution of the procedures estimating functional or effective cortical source connectivity from rsEEG rhythms is an open issue for basic research, but high-resolution EEG approaches are recommended to explore *default mode*, frontoparietal *attentional*, and other established cortical neural networks (Teipel et al., 2016). However, high-resolution EEG techniques may under-evaluate cortical sources buried in the inter-hemispherical fissure such as those of the *default mode network* (i.e., medial prefrontal, cingulate, and precuneus).

When the rsEEG source connectivity is calculated, both inter- and intra-hemispherical analyses are recommended. For the inter-hemispherical analysis, the rsEEG source connectivity can be calculated between all (equivalent current) dipoles of the mentioned cortical regions of interest for each hemisphere with the corresponding ones of the other hemisphere. The rsEEG source connectivity solutions for all dipoles of a given pair of cortical regions of interest are typically averaged. For the intra-hemispherical analysis, the rsEEG source connectivity estimates are computed for all dipoles of a cortical region of interest with all dipoles of another cortical region of interest in the same hemisphere. The rsEEG source connectivity solutions for all dipoles of a given pair of cortical regions of interest are then averaged.

6.5. The issue of cortical tangential sources

One should keep in mind the example of Fig. 1 (upper row) in the critical evaluation of any solution obtained by both (1) EEG source estimation techniques modeling cortical sources and head volume conductor, and (2) those based on Laplacian estimation or the solution of the inner continuation problem. In the figure, a given cortical source oriented tangentially to the scalp surface (e.g., sources located in cortical sulci and fissures) generates neural electric fields spreading relatively far from the scalp sensor overlying that source (10–12 cm; Srinivasan et al., 2007). As mentioned above, these neural electric fields would be conducted to distant scalp electrodes and could be erroneously interpreted as due to underlying cortical radial sources.

6.6. The number of electrodes for the spatial analysis of rsEEG rhythms

There is no consensus on the minimum number of scalp electrodes to be used for the spatial analysis of the rsEEG rhythms by "synchronization" and "connectivity" features. In the past years, these techniques have repeatedly been used in neurological subjects in whom rsEEG rhythms were recorded from 19 electrodes placed according to 10–20 system (Riba et al., 2004; Huang et al., 2000; Mulert et al., 2001; Winterer et al., 2001; Babiloni et al., 2004, 2006, 2015, 2016b; Veiga et al., 2003; Hata et al., 2016). Indeed, these rsEEG rhythms are generated by largely distributed cerebral networks that may mitigate inaccuracy and spatial aliasing in the source estimation based on the 10–20 system when large cortical regions of interest are used. Source estimations based on the 10–20 system may be limited to existing rsEEG databases for the exploratory testing of proof-of-concepts in retrospective studies. Findings of those retrospective studies should be cross-validated and extended by studies based on *high-resolution EEG* techniques, defined as the experimental procedures using ≥48–64 (until 128–256) electrodes and cortical source mapping including the computation of (1) brain source estimates, (2) scalp current density (surface Laplacian transformation), and (3) dura surface potential based on mathematical models of head volume conductor.

A high number of electrodes in the rsEEG recordings is welcome on the condition that the quality of the experimental procedure is good enough, namely an equal and low impedance (<5–10 KΩ) in all electrodes used for the final rsEEG source estimation. The higher the number of electrodes, the smaller the regions of interest in the rsEEG source estimation. In particular, high-resolution EEG techniques are recommended to probe cortical neural networks showing a correlation between blood oxygen level-dependent (BOLD) activity recorded during rs-fMRI and rsEEG rhythms (Goncalves et al., 2006; Jann et al., 2010; Mantini et al., 2007). These studies found that power fluctuation of rsEEG rhythms are correlated with BOLD signal fluctuations in the thalamus (Goncalves et al., 2006) and cortical regions including the default mode network (Mantini et al., 2007; Jann et al., 2010).

7. Statistical analysis and interpretation of scalp rsEEG variables

7.1. Statistical analysis of rsEEG variables

In clinical research, main statistical analyses of rsEEG variables include (1) the preliminary computation of the sample size to determine the adequate number of subjects for any experimental group of an experiment as a function of the desired statistical power (a significant effect may not be observed due to an insufficient sample size); (2) comparison of the means between subjects belonging to disease and control groups; (3) correlation of those variables with relevant clinical and neuropathological disease markers across patients; (4) the classification of individuals of two groups (i.e. disease and control); and (5) the belonging of a single patient to a control group. For these statistical analyses, we recommend a particular care to the following aspects.

First, reproducibility of values of a given rsEEG variable should be tested in at least two periods lasting a minimum of 1 minute of artifact-free rsEEG epochs (even non-consecutive) for any experimental condition. At the individual level, the variable values should be (1) similar in each period and (2) consistent at more than one scalp recording site or source. At the group level, the variable values should not statistically differ between the two periods at more than one scalp recording site or source at the desired statistical threshold.

Second, the measured value of reproducible individual rsEEG variables can be compared with normative databases of healthy controls or pathological groups as a preliminary test of an underlying pathological condition (see as examples procedure using rsEEG variables derived from scalp and source spaces; Szava et al., 1994; Bosch-Bayard et al., 2001). For this analysis, pathological groups may include not only the group of patients with the disease of interest but also control disease groups to test the specificity of experimental results. At the group level, such rsEEG variables can be compared between cohorts of healthy controls, patients of the disease of interest, and patients with a control disease. If such rsEEG variables were able to distinguish the disease group of interest from the other ones, the discriminant rsEEG variables should be cross-validated in independent groups before final conclusions. However, a statistical abnormality of rsEEG variables is not necessarily indicative of a pathological condition. Eventual statistical differences may be merely due to confounding factors including age, education, inter-subject genetic variability (e.g., BDNF, COMT), past major neurological and psychiatric diseases, past historical brain infections, an agitated night's sleep before the recording day, drowsiness, non-annotated emotional reactions or environmental noise during the EEG recording, psychoactive substances (e.g., coffee, tea, psychoactive medications), and skull defects.

Third, statistical analyses should consider false positive findings due to multiple comparisons.

Noteworthy, commercial tools and databases of potential interest for clinical research are available to test normality of rsEEG variables with z-scores expressed as a significance probability mapping or other statistical analyses. The outcome of those procedures should be evaluated with caution due to, for example, predisposition for false positives, statistical assumptions, development with a given set of equipment but application on other sets of equipment, and the limited access of users and researchers to more methodological and technical details for careful evaluation and independent cross-validation testing.

7.2. Interpretation of rsEEG variables

In clinical research, results of the rsEEG frequency and topographical analysis should be interpreted with great caution and in-depth expert knowledge. We recommend some precautions in communicating those results in any scientific report or dissemination activity. The Authors of a scientific study should make clear and distinct: (1) the specific *clinical hypothesis* at the basis of any kind of frequency or topographical analysis of rsEEG rhythms (clinical or not); (2) the methodological *assumptions* at the base of the techniques used for the analysis of the frequency and topography of rsEEG data at sensor or source level; (3) the study *results* (in terms of specific rsEEG variables and their statistical associations); (4) the *interpretation of the results in terms of neurophysiological/biophysical models of cortical activity and connectivity* based on quoted previous evidence and explicit theoretical speculations; and (5) any *new hypothesis* generated on the basis of the results.

8. Overview and concluding remarks

As mentioned above, in the present study the term "clinical research" is strictly related to experimental studies in patients with neurological and psychiatric diseases, so the following concluding remarks may not pertain to methodological procedures and terms used in the daily medical practice supplied in services of Clinical Neurophysiology.

First, recording of rsEEG rhythms is an experiment on brain neurophysiological mechanisms underpinning the control and maintenance of cerebral arousal and vigilance in quiet wakefulness. As mentioned above, the instructions to the subject can vary as a function of the specific research interest, namely the neural basis of rapid brain reactivity to eyes opening/closing or the maintenance of quiet wakefulness with eyes closed for several minutes. We recommend controlling environmental conditions and to instruct the subject in a repeatable way to compare results in cross-modal and longitudinal clinical studies.

Second, we recommend the use of high-resolution EEG techniques (up to 128–256 electrodes and more than one referential electrode) to enhance spatial information content in cortical topographic mapping. The use of these techniques implies a careful balance of the impedance in all scalp electrodes to ensure the good quality of EEG recordings. EKG (e.g., heart rate variability), EMG, and skin galvanic resistance (or skin conductance) should be used to monitor brain arousal underlying rsEEG rhythms.

Third, fixed EEG frequency bands should be used only if the IAF peak of patients did not differ from that of control subjects. In case of a frequency slowing in that peak in patients, the frequency bands should be adjusted on an individual basis in all subjects.

Fourth, two broad classes of rsEEG features can be arbitrarily derived from frequency analysis. The "synchronization" features (e.g., amplitude/power density spectrum, etc.) might reflect underlying local mechanisms of synchronization of cortical neurons at different frequencies, generating rsEEG activity. The "connectivity" features (e.g., spectral coherence, etc.) might probe either the interdependence of recorded or transformed (i.e., surface Laplacian or inner continuation inverse problem) rsEEG rhythms at the electrode level or the rsEEG source connectivity. The former may be biased by head volume conduction effects, while the latter just approximates real head volume conduction properties and lacks a unique solution. We recommend to cross-validate the results using more than one technique for each class of those features.

Fifth, compared to the mentioned procedures of time-frequency analysis, matching pursuit decomposition presents some advantages, even for multivariate datasets and EEG source estimation.

Sixth, the first preliminary step of the rsEEG nonlinear data analysis should confirm if these data display nonlinearity or determinism. If affirmative, a promising research approach for future clinical research is the comparison of several linear and nonlinear

measurements to understand their value and neurophysiological underpinnings.

Seventh, we recommend more international cooperation among the experts of frequency and topographical analysis of rsEEG variables to create a public repository for the following contents that would be very useful in clinical research: (1) shared software tools for the computation of the above "synchronization" and "connectivity" features of rsEEG rhythms. They may allow consensus studies about the effects of volume conduction, common drive, and cascade flow on the validity and reliability of the frequency and topographical analysis of the rsEEG variables at sensor and source levels (see Fig. 1); (2) real rsEEG data collected in groups of healthy and neurological subjects. Ideally, the solutions of the rsEEG frequency and topographical analysis should be compared to the scalp, modeled dura mater, and modeled cortical sources. The findings of such an international initiative may represent a reference for a future public consensus on the use of the different techniques of rsEEG frequency and topographical analysis in clinical research.

Declaration of Competing Interest

The authors declared that there is no conflict of interest.

Acknowledgements

References

Aru J, Aru J, Priesemann V, Wibral M, Lana L, Pipa G, et al. Untangling cross-frequency coupling in neuroscience. Curr Opin Neurobiol 2015;31:51–61.

Babiloni C, Binetti G, Cassetta E, Cerboneschi D, Dal Forno G, Del Percio C, et al. Mapping distributed sources of cortical rhythms in mild Alzheimers disease. A multi-centric EEG study. Neuroimage 2004;22:57–67.

Babiloni C, Benussi L, Binetti G, Bosco P, Busonero G, Cesaretti S, et al. Genotype (cystatin C) and EEG phenotype in Alzheimer disease and mild cognitive impairment: a multicentric study. Neuroimage 2006;29(3):948–64.

Babiloni C, Del Percio C, Boccardi M, Lizio R, Lopez S, Carducci F, et al. Occipital sources of resting-state alpha rhythms are related to local gray matter density in subjects with amnesic mild cognitive impairment and Alzheimer's disease. Neurobiol Aging 2015;36:556–70.

Babiloni C, Lizio R, Vecchio F, Frisoni GB, Pievani M, Geroldi C, et al. Reactivity of cortical alpha rhythms to eye opening in mild cognitive impairment and Alzheimer's disease: an EEG study. J Alzheimers Dis 2010;22:1047–64.

Babiloni C, Lizio R, Marzano N, Capotosto P, Soricelli A, Triggiani AI, et al. Brain neural synchronization and functional coupling in Alzheimer's disease as revealed by resting state EEG rhythms. Int J Psychophysiol 2016a;103:88–102.

Babiloni F, Cincotti F, Carducci F, Rossini PM, Babiloni C. Spatial enhancement of EEG data by surface Laplacian estimation: the use of magnetic resonance imaging-based head models. Clin Neurophysiol 2001;112:724–7.

Babiloni C, Del Percio C, Caroli A, Salvatore E, Nicolai E, Marzano N, et al. Cortical sources of resting state EEG rhythms are related to brain hypometabolism in subjects with Alzheimer's disease: an EEG-PET study. Neurobiol Aging 2016b;48:122–34.

Baccalá LA, Sameshima K. Partial directed coherence: a new concept in neural structure determination. Biol Cybern 2001;84:463–74.

Baillet S, Friston K, Oostenveld R. Academic software applications for electromagnetic brain mapping using MEG and EEG. Comput Intell Neurosci. 2011;2011:972050.

Barry RJ, Clarke AR, Johnstone SJ. Caffeine and opening the eyes have additive effects on resting arousal measures. Clin Neurophysiol 2011;122:2010–5.

Barry RJ, De Blasio FM. EEG differences between eyes-closed and eyes-open resting remain in healthy ageing. Biol Psychol 2017;129:293–304.

Başar E. A review of alpha activity in integrative brain function: fundamental physiology, sensory coding, cognition and pathology. Int J Psychophysiol 2012;86:1–24.

Başar E. A review of gamma oscillations in healthy subjects and in cognitive impairment. Int J Psychophysiol 2013;90:99–117.

Bassett DS, Bullmore E. Small-world brain networks. Neuroscientist 2006;12:512–23.

Bassett DS, Meyer-Lindenberg A, Achard S, Duke T, Bullmore E. Adaptive reconfiguration of fractal small-world human brain functional networks. Proc Natl Acad Sci U S A 2006;103:19518–23.

Bénar CG, Papadopoulo T, Torrésani B, Clerc M. Consensus Matching Pursuit for multi-trial EEG signals. J Neurosci Methods 2009;180:161–70.

Beniczky S, Aurlien H, Brøgger JC, Hirsch LJ, Schomer DL, Trinka E, et al. Standardized computer-based organized reporting of EEG: SCORE – second version. Clin Neurophysiol 2017;128:2334–46.

Bergmann TO, Karabanov A, Hartwigsen G, Thielscher A, Siebner HR. Combining non-invasive transcranial brain stimulation with neuroimaging and electrophysiology: current approaches and future perspectives. Neuroimage 2016;140:4–19.

Billings SA. Nonlinear system identification: NARMAX methods in the time, frequency, and spatio-temporal domains. John Wiley & Sons; 2013.

Blanco S, Garcia H, Quiroga RQ, Romanelli L, Rosso OA. Stationarity of the EEG series. IEEE Eng Med Biol Mag 1995;14:395–9.

Blinowska KJ, Zygierewicz J. Practical biomedical signal analysis. CRC Press; 2012.

Blinowska KJ. Review of the methods of determination of directed connectivity from multichannel data. Med Biol Eng Comput 2011;49:521–9.

Blinowska KJ, Kaminski M. Functional brain networks: random, "small world" or deterministic? PLoS One 2013;8:e78763.

Blinowska KJ, Rakowski F, Kaminski M, De Vico Fallani F, Del Percio C, Lizio R, et al. Functional and effective brain connectivity for discrimination between Alzheimer's patients and healthy individuals: a study on resting state EEG rhythms. Clin Neurophysiol 2017;128:667–80.

Boccaletti S, Valladares DL, Pecora LM, Geffert HP, Carroll T. Reconstructing embedding spaces of coupled dynamical systems from multivariate data. Phys Rev E Stat Nonlin Soft Matter Phys 2002;65:035204.

Bodenmann S, Rusterholz T, Dürr R, Stoll C, Bachmann V, Geissler E, et al. The functional Val158Met polymorphism of COMT predicts interindividual differences in brain alpha oscillations in young men. J Neurosci 2009;29:10855–62.

Bosch-Bayard J, Valdes-Sosa P, Virues-Alba T, Aubert-Vazquez E, John ER, Harmony T, et al. 3D statistical parametric mapping of EEG source spectra by means of variable resolution electromagnetic tomography (VARETA). Clin Electroencephalogr 2001;32:47–61.

Bosch-Bayard J, Valdés-Sosa PA, Fernandez T, Otero G, Pliego Rivero B, Ricardo-Garcell J, et al. 3D statistical parametric mapping of quiet sleep EEG in the first year of life. Neuroimage 2012;59:3297–308.

Brazier MA. Spread of seizure discharges in epilepsy: anatomical and electrophysiological considerations. Exp Neurol 1972;36:263–72.

Breakspear M, Terry JR. Detection and description of non-linear interdependence in normal multichannel human EEG data. Clin Neurophysiol 2002;113:735–53.

Brunner C, Billinger M, Seeber M, Mullen TR, Makeig S. Volume conduction influences scalp-based connectivity estimates. Front Comput Neurosci 2016;10:121.

Canolty RT, Edwards E, Dalal SS, Soltani M, Nagarajan SS, Kirsch HE, et al. High gamma power is phase-locked to theta oscillations in human neocortex. Science 2006;313:1626–8.

Canolty RT, Knight RT. The functional role of cross-frequency coupling. Trends Cogn Sci 2010;14:506–15.

Capotosto P, Babiloni C, Romani GL, Corbetta M. Frontoparietal cortex controls spatial attention through modulation of anticipatory alpha rhythms. J Neurosci 2009;29:5863–72.

Capotosto P, Babiloni C, Romani GL, Corbetta M. Resting-state modulation of α rhythms by interference with angular gyrus activity. J Cogn Neurosci 2014;26:107–19.

Chand GB, Wu J, Hajjar I, Qiu D. Interactions of the salience network and its subsystems with the default-mode and the central-executive networks in normal aging and mild cognitive impairment. Brain Connect 2017;7:401–12.

Chandran KSS, Mishra A, Shirhatti V, Ray S. Comparison of matching pursuit algorithm with other signal processing techniques for computation of the time-frequency power spectrum of brain signals. J Neurosci 2016;36:3399–408.

Chella F, Pizzella V, Zappasodi F, Marzetti L. Impact of the reference choice on scalp EEG connectivity estimation. J Neural Eng 2016;13:036016.

Cohen MX, Elger CE, Fell J. Oscillatory activity and phase-amplitude coupling in the human medial frontal cortex during decision making. J Cogn Neurosci 2009;21:390–402.

Cole SR, van der Meij R, Peterson EJ, de Hemptinne C, Starr PA, Voytek B. Nonsinusoidal beta oscillations reflect cortical pathophysiology in parkinson's disease. J Neurosci 2017;37:4830–40.

D'Amelio M, Rossini PM. Brain excitability and connectivity of neuronal assemblies in Alzheimer's disease: from animal models to human findings. Prog Neurobiol 2012;99:42–60.

Damoiseaux JS, Greicius MD. Greater than the sum of its parts: a review of studies combining structural connectivity and resting-state functional connectivity. Brain Struct Funct 2009;213:525–33.

Damoiseaux JS, Rombouts SA, Barkhof F, Scheltens P, Stam CJ, Smith SM, et al. Consistent resting-state networks across healthy subjects. Proc Natl Acad Sci U S A 2006;103:13848–53.

Darmani G, Zipser CM, Böhmer GM, Deschet K, Müller-Dahlhaus F, Belardinelli P, et al. Effects of the selective α5-GABAAR antagonist S44819 on excitability in the human brain: a TMS-EMG and TMS-EEG phase I study. J Neurosci 2016;36:12312–20.

Dauvilliers Y, Tafti M, Landolt HP. Catechol-O-methyltransferase, dopamine, and sleep-wake regulation. Sleep Med Rev 2015;22:47–53.

Dauwels J, Vialatte F, Musha T, Cichocki A. A comparative study of synchrony measures for the early diagnosis of Alzheimer's disease based on EEG. Neuroimage 2010;49:668–93.

David O, Kiebel SJ, Harrison LM, Mattout J, Kilner JM, Friston KJ. Dynamic causal modeling of evoked responses in EEG and MEG. Neuroimage 2006;30:1255–72.

Demiralp T, Bayraktaroglu Z, Lenz D, Junge S, Busch NA, Maess B, et al. Gamma amplitudes are coupled to theta phase in human EEG during visual perception. Int J Psychophysiol 2007;64:24–30.

Durka P, Blinowska KJ. Analysis of EEG transients by means of matching pursuit. Ann Biomed Eng 1995;23:608–11.

Durka PJ, Matysiak A, Martinez-Montes E, Valdes Sosa P, Blinowska KJ. Multichannel matching pursuit and EEG inverse solutions. J Neurosci Methods 2005;148:49–59.

Durka PJ, Malinowska U, Zieleniewska M, O'Reilly C, Różański PT, Żygierewicz J. Spindles in Svarog: framework and software for parametrization of EEG transients. Front Hum Neurosci 2015;9:258.

Eckman JP, Ruelle D. Fundamental limitations for estimating dimensions and Lyapunov exponents in dynamical systems. Physica D 1992;56:185–7.

Engel Jr J, da Silva FL. High-frequency oscillations – where we are and where we need to go. Prog Neurobiol 2012;98:316–8.

Faure P, Korn H. Is there chaos in the brain? I. Concepts of nonlinear dynamics and methods of investigation. C R Acad Sci 2001;III(324):773–93.

Fingelkurts AA, Fingelkurts AA. EEG oscillatory states: universality, uniqueness and specificity across healthy-normal, altered and pathological brain conditions. PLoS One 2014;9:e87507.

Fingelkurts AA, Fingelkurts AA. Timing in cognition and EEG brain dynamics: discreteness versus continuity. Cogn Process 2006;7:135–62.

Fraschini M, Demuru M, Crobe A, Marrosu F, Stam CJ, Hillebrand A. The effect of epoch length on estimated EEG functional connectivity and brain network organisation. J Neural Eng 2016;13:036015.

Fries P. Rhythms for cognition: communication through coherence. Neuron 2015;88:220–35.

Friston K, Moran R, Seth AK. Analysing connectivity with Granger causality and dynamic causal modelling. Curr Opin Neurobiol 2013;23:172–8.

Friston KJ. Functional and effective connectivity: a review. Brain Connect 2011;1:13–36.

Friston KJ, Holmes AP, Worsley KJ, Poline JP, Frith CD, Frackowiak RSJ. Statistical parametric maps in functional imaging: a general linear approach. Hum Brain Mapp 1994;2:189–210.

Goncalves SI, de Munck JC, Pouwels PJ, Schoonhoven R, Kuijer JP, Maurits NM, et al. Correlating the alpha rhythm to BOLD using simultaneous EEG/fMRI: inter-subject variability. Neuroimage 2006;30:203–13.

Gramfort A, Strohmeier D, Haueisen J, Hämäläinen MS, Kowalski M. Time-frequency mixed-norm estimates: sparse M/EEG imaging with non-stationary source activations. Neuroimage 2013;70:410–22.

Granger CWJ. Investigating causal relations in by econometric models and cross-spectral methods. Econometrica 1969;37:424–1348.

Gratton G, Villa AE, Fabiani M, Colombis G, Palin E, Bolcioni G, et al. Functional correlates of a three-component spatial model of the alpha rhythm. Brain Res 1992;582:159–62.

Guindalini C, Mazzotti DR, Castro LS, D'Aurea CV, Andersen ML, Poyares D, et al. Brain-derived neurotrophic factor gene polymorphism predicts interindividual variation in the sleep electroencephalogram. J Neurosci Res 2014;92:1018–23.

Güntekin B, Başar E. Review of evoked and event-related delta responses in the human brain. Int J Psychophysiol 2016;103:43–52.

Hata M, Kazui H, Tanaka T, Ishii R, Canuet L, Pascual-Marqui RD, et al. Functional connectivity assessed by resting state EEG correlates with cognitive decline of Alzheimer's disease – an eLORETA study. Clin Neurophysiol 2016;127:1269–78.

He P, Wilson G, Russell C. Removal of ocular artifacts from electro- encephalogram by adaptive filtering. Med Biol Eng Comput 2004;42:407–12.

Helfrich RF, Knight RT. Oscillatory dynamics of prefrontal cognitive control. Trends Cogn Sci 2016;20:916–30.

Hernandez JL, Valdes PA, Vila P, Valdes P. EEG spike and wave modelled by a stochastic limit cycle. Neuroreport 1996;7:2246–50.

Hirsch LJ, LaRoche SM, Gaspard N, Gerard E, Svoronos A, Herman ST, et al. American clinical neurophysiology society's standardized critical care EEG terminology: 2012 version. J Clin Neurophysiol. 2013;30:1–27.

Hjorth B. Principles for transformation of scalp EEG from potential field into source distribution. J Clin Neurophysiol 1991;8:391–6.

Hlaváčková-Schindler K, Paluš M, Vejmelka M, Bhattacharya J. Causality detection based on information-theoretic approaches in time series analysis. Phys Rep 2007;441:1–46.

Hlinka J, Hartman D, Jajcay N, Tomecek D, Tintera J, Palus M. Small-world bias of correlation networks: From brain to climate. Chaos 2017;27:035812.

Huang C, Wahlund L, Dierks T, Julin P, Winblad B, Jelic V. Discrimination of Alzheimer's disease and mild cognitive impairment by equivalent EEG sources: a cross-sectional and longitudinal study. Clin Neurophysiol 2000;111:1961–7.

Huang L, Yu P, Ju F, Cheng J. Prediction of response to incision using the mutual information of electroencephalograms during anaesthesia. Med Eng Phys 2003;25:321–7.

Isaksson A, Wennberg A, Zetterberg LH. Computer analysis of EEG signals with parametric models. Proc IEEE 1981;69:451–61.

Jann K, Koenig T, Dierks T, Boesch C, Federspiel A. Association of individual resting state EEG alpha frequency and cerebral blood flow. Neuroimage 2010;51:365–72.

Jansen BH, Agarwal G, Hegde A, Boutros NN. Phase synchronization of the ongoing EEG and auditory EP generation. Clin Neurophysiol 2003;114:79–85.

Jensen O, Spaak E, Park H. Discriminating valid from spurious indices of phase-amplitude coupling. eNeuro 2017;3.

Jeong J, Chae JH, Kim SY, Han SH. Nonlinear dynamic analysis of the EEG in patients with Alzheimer's disease and vascular dementia. J Clin Neurophysiol 2001a;18:58–67.

Jeong J, Gore JC, Peterson BS. Mutual information analysis of the EEG in patients with Alzheimer's disease. Clin Neurophysiol 2001b;112:827–35.

Jeong J, Kim DJ, Chae JH, Kim SY, Ko HJ, Paik IH. Nonlinear analysis of the EEG of schizophrenics with optimal embedding dimension. Med Eng Phys 1998a;20:669–76.

Jeong J, Kim MS, Kim SY. Test for low-dimensional determinism in electroencephalograms. Phys Rev E Stat Phys Plasmas Fluids Relat Interdiscip Top 1999;60:831–7.

Jeong J, Kim SY, Han SH. Non-linear dynamical analysis of the EEG in Alzheimer's disease with optimal embedding dimension. Electroencephalogr Clin Neurophysiol 1998b;106:220–8.

Jeong J. EEG dynamics in patients with Alzheimer's disease. Clin Neurophysiol 2004;115:1490–505.

Jobert M, Wilson FJ, Ruigt GS, Brunovsky M, Prichep LS, Drinkenburg WH, et al. Guidelines for the recording and evaluation of pharmaco-EEG data in man: the International Pharmaco-EEG Society (IPEG). Neuropsychobiology 2012;66:201–20.

Kaminski M, Blinowska KJ. The influence of volume conduction on DTF estimate and the problem of its mitigation. Front Comput Neurosci 2017;11:36.

Kamiński MJ, Blinowska KJ. A new method of the description of the information flow in the brain structures. Biol Cybern 1991;65:203–10.

Kane N, Acharya J, Benickzy S, Caboclo L, Finnigan S, Kaplan PW, et al. A revised glossary of terms most commonly used by clinical electroencephalographers and updated proposal for the report format of the EEG findings. Revision 2017. Clin Neurophysiol Pract 2017;2:170–85.

Kanz H, Schreiber T. Nonlinear time series analysis. Cambridge: Cambridge University Press; 1997.

Kaplan AY, Fingelkurts AA, Fingelkurts AA, Borisov SV, Darkhovsky BS. Nonstationary nature of the brain activity as revealed by EEG/MEG: methodological, practical and conceptual challenges. Signal Process 2005;85:2190–212.

Karahan E, Rojas-Lopez PA, Bringas-Vega ML, Valdes-Hernandez PA, Valdes-Sosa PA. Tensor analysis and fusion of multimodal brain images. Proc IEEE. 2015;103:1531–49.

Kayser J, Tenke CE. Issues and considerations for using the scalp surface Laplacian in EEG/ERP research: a tutorial review. Int J Psychophysiol 2015;97:189–209.

Khanna A, Pascual-Leone A, Michel CM, Farzan F. Microstates in resting-state EEG: current status and future directions. Neurosci Biobehav Rev 2015;49:105–13.

Keil A, Debener S, Gratton G, Junghöfer M, Kappenman ES, Luck SJ, et al. Committee report: publication guidelines and recommendations for studies using electroencephalography and magnetoencephalography. Psychophysiology 2014;51:1–21.

Khlif MS, Colditz PB, Boashash B. Effective implementation of time-frequency matched filter with adapted pre and postprocessing for data-dependent detection of newborn seizures. Med Eng Phys 2013;35:1762–9.

Kim DJ, Jeong J, Chae JH, Park S, Yong Kim S, Jin Go H, et al. An estimation of the first positive Lyapunov exponent of the EEG in patients with schizophrenia. Psychiatry Res 2000;98:177–89.

Klimesch W, Doppelmayr M, Russegger H, Pachinger T, Schwaiger J. Induced alpha band power changes in the human EEG and attention. Neurosci Lett 1998;244:73–6.

Klimesch W, Sauseng P, Hanslmayr S, Gruber W, Freunberger R. Event-related phase reorganization may explain evoked neural dynamics. Neurosci Biobehav Rev 2007;31:1003–16.

Klimesch W. EEG alpha and theta oscillations reflect cognitive and memory performance: a review and analysis. Brain Res Rev 1999;29:169–95.

Klimesch W. Alpha-band oscillations, attention, and controlled access to stored information. Trends Cogn Sci 2012;16:606–17.

Klimesch W. An algorithm for the EEG frequency architecture of consciousness and brain body coupling. Front Hum Neurosci 2013;7:766.

Korn H, Faure P. Is there chaos in the brain? II. Experimental evidence and related models. C R Biol 2003;326:787–840.

Kullback S. Information theory and statistics. John Wiley & Sons; 1959.

Kuś R, Kamiński M, Blinowska KJ. Determination of EEG activity propagation: pairwise versus multichannel estimate. IEEE Trans Biomed Eng 2004;51:1501–10.

Latchoumane CF, Jeong J. Quantification of brain macrostates using dynamical nonstationarity of physiological time series. IEEE Trans Biomed Eng 2011;58:1084–93.

Le Van Quyen M, Adam C, Baulac M, Martinerie J, Varela FJ. Nonlinear interdependencies of EEG signals in human intracranially recorded temporal lobe seizures. Brain Res 1998;792:24–40.

Lei X, Liao K. Understanding the influences of EEG reference: a large-scale brain network perspective. Front Neurosci 2017;11:205.

Lehmann D, Ozaki H, Pal I. EEG alpha map series: brain micro-states by space-oriented adaptive segmentation. Electroenceph Clin Neurophysiol 1987;67:271–88.

Leuchter AF, Cook IA, Newton TF, Dunkin J, Walter DO, Rosenberg-Thompson S, et al. Regional differences in brain electrical activity in dementia: use of spectral power and spectral ratio measures. Electroencephalogr Clin Neurophysiol 1993;87:385–93.

Lopes da Silva FH. Computer-assisted EEG diagnosis: pattern recognition and brain mapping. In: Schomer DL, Lopes da Silva FH, editors. Niedermeyer's electroencephalography basic principles, clinical applications and related fields. 6th ed. Philadelphia: Lippincott Williams & Wilkins; 2011. p. 1203–26.

Lopes da Silva FH, Pijn JP, Velis D, Nijssen PC. Alpha rhythms: noise, dynamics and models. Int J Psychophysiol 1997;26:237–49.

Lopes da Silva FH, Pijn JP, Wadman WJ. Dynamics of local neuronal networks: control parameters and state bifurcations in epileptogenesis. In: van Pelt J, Comer MA, Uylings HBM, Lopes da Silva FH, editors. Progress in brain research 1994;vol. 102. Amsterdam: Elsevier; 1994. p. 359–70.

Lopes da Silva F. EEG and MEG: relevance to neuroscience. Neuron 2013;80:1112–28.

Mahjoory K, Nikulin VV, Botrel L, Linkenkaer-Hansen K, Fato MM, Haufe S. Consistency of EEG source localization and connectivity estimates. Neuroimage 2017;152:590–601.

Malinowska U, Klekowicz H, Wakarow A, Niemcewicz S, Durka PJ. Fully parametric sleep staging compatible with the classical criteria. Neuroinformatics 2009;7:245–53.

Mallat SG, Zhang Z. Matching pursuit with time-frequency dictionaries. IEEE Trans Signal Process 1993;1993(41):3397–415.

Mantini D, Perrucci MG, Del Gratta C, Romani GL, Corbetta M. Electrophysiological signatures of resting state networks in the human brain. Proc Natl Acad Sci U S A 2007;104:13170–5.

Mars NJ, Thompson PM, Wilkus RJ. Spread of epileptic seizure activity in humans. Epilepsia 1985;26:85–94.

McKeith IG, Dickson DW, Lowe J, Emre M, O'Brien JT, Feldman H, et al. Diagnosis and management of dementia with Lewy bodies: third report of the DLB Consortium. Neurology 2005;65:1863–72.

McKeith IG, Boeve BF, Dickson DW, Halliday G, Taylor JP, Weintraub D, et al. Diagnosis and management of dementia with Lewy bodies: Fourth consensus report of the DLB Consortium. Neurology 2017;89:88–100.

Medaglia JD. Graph theoretic analysis of resting state functional MR imaging. Neuroimaging Clin N Am 2017;27:593–607.

Miocinovic S, de Hemptinne C, Qasim S, Ostrem JL, Starr PA. Patterns of cortical synchronization in isolated dystonia compared with parkinson disease. JAMA Neurol 2015;72:1244–51.

Michel CM, Koenig T. EEG microstates as a tool for studying the temporal dynamics of whole-brain neuronal networks: a review. Neuroimage 2018;180:577–93.

Moretti DV, Babiloni F, Carducci F, Cincotti F, Remondini E, Rossini PM, et al. Computerized processing of EEG–EOG–EMG artifacts for multicentric studies in EEG oscillations and event-related potentials. Int J Psychophysiol 2003;47:199–216.

Mosher JC, Baillet S, Leahy RM. EEG source localization and imaging using multiple signal classification approaches. J Clin Neurophysiol 1999;16:225–38.

Mukamel EA, Wong KF, Prerau MJ, Brown EN, Purdon PL. Phase-based measures of cross-frequency coupling in brain electrical dynamics under general anesthesia. Conf Proc IEEE Eng Med Biol Soc 2011;2011:1981–4.

Mulert C, Gallinat J, Pascual-Marqui R, Dorn H, Frick K, Schlattmann P, et al. Reduced event-related current density in the anterior cingulate cortex in schizophrenia. Neuroimage 2001;13:589–600.

Na SH, Jin SH, Kim SY, Ham BJ. EEG in schizophrenic patients: mutual information analysis. Clin Neurophysiol 2002;113:1954–60.

Netoff T, Caroll I, Pecora LM, Schiff SJ. Detecting coupling in the presence of noise and nonlinearity. In: Schelter B, Winterhalder M, Timmer J, editors. Handbook of time series analysis. Wiley VCH; 2006.

Neuper C, Wörtz M, Pfurtscheller G. ERD/ERS patterns reflecting sensorimotor activation and deactivation. Prog Brain Res 2006;159:211–22.

Nichols TE, Das S, Eickhoff SB, Evans AC, Glatard T, Hanke M, et al. Best practices in data analysis and sharing in neuroimaging using MRI. Nat Neurosci 2017;20:299–303.

Nilsson J, Panizza M, Hallett M. Principles of digital sampling of a physiologic signal. Electroencephalogr Clin Neurophysiol 1993;89:349–58.

Nolte G, Bai O, Wheaton L, Mari Z, Vorbach S, Hallett M. Identifying true brain interaction from EEG data using the imaginary part of coherency. Clin Neurophysiol 2004;115:2292–307.

Nunez PL, Srinivasan R. Electric fields of the brain: the neurophysics of EEG. 2nd ed. New York: Oxford University Press; 2006.

Nunez PL. Estimation of large scale neocortical source activity with EEG surface Laplacians. Brain Topogr 1989;2:141–54.

Nunez PL. REST: A good idea but not the gold standard. Clin Neurophysiol 2010;121:2177–80.

Nunez PL. Toward a quantitative description of large-scale neocortical dynamic function and EEG. Behav Brain Sci 2000;23:371–98.

Nunez PL. A brief history of the EEG surface Laplacian; 2012 http://ssltool.sourceforge.net/history.html.

Nuwer MR, Comi G, Emerson R, Fuglsang-Frederiksen A, Guérit JM, Hinrichs H, Ikeda A, Luccas FJ, Rappelsburger P. IFCN standards for digital recording of clinical EEG. Int Fed Clin Neurophys Electroencephalogr Clin Neurophysiol 1998;106:259–61.

Nuwer MR, Lehmann D, da Silva FL, Matsuoka S, Sutherling W, Vibert JF. IFCN guidelines for topographic and frequency analysis of EEGs and EPs. Int Fed Clin Neurophys Electroencephalogr Clin Neurophysiol Suppl 1999;52:15–20.

Osborne AR, Provenzale A. Finite correlation dimension for stochastic systems with power-law spectra. Physica D 1989;35:357–81.

Osipova D, Hermes D, Jensen O. Gamma power is phase-locked to posterior alpha activity. PloS One 2008;3:e3990.

Oswal A, Brown P, Litvak V. Movement related dynamics of subthalmo-cortical alpha connectivity in Parkinson's disease. Neuroimage 2013a;70:132–42.

Oswal A, Brown P, Litvak V. Synchronized neural oscillations and the pathophysiology of Parkinson's disease. Curr Opin Neurol 2013b;26:662–70.

Papo D, Zanin M, Martinez JH, Buldu JM. Beware of Small-world neuroscientist! Front Hum Neurosci 2016;10:96.

Pardey J, Roberts S, Tarassenko L. A review of parametric modelling techniques for EEG analysis. Med Eng Phys 1996;18:2–11.

Pascual-Marqui RD, Biscay RJ, Bosch-Bayard J, Lehmann D, Kochi K, Kinoshita T, et al. Assessing direct paths of intracortical causal information flow of oscillatory activity with the isolated effective coherence (iCoh). Front Hum Neurosci 2014;8:448.

Pascual-Marqui RD, Esslen M, Kochi K, Lehmann D. Functional imaging with low resolution brain electromagnetic tomography (LORETA): a review. Methods Find Exp Clin Pharmacol 2002;24:91–5.

Pascual-Marqui RD, Gonzalez-Andino SL, Valdes-Sosa PA. Current source density estimation and interpolation based on the spherical harmonic Fourier expansion. Int J Neurosci 1988a;43:237–49.

Pascual-Marqui RD, Lehmann D, Koukkou M, Kochi K, Anderer P, Saletu B, et al. Assessing interactions in the brain with exact low-resolution electromagnetic tomography. Philos Trans A Math Phys Eng Sci 2011;369:3768–84.

Pascual-Marqui RD, Valdes-Sosa PA, Alvarez-Amador A. A parametric model for multichannel EEG spectra. Int J Neurosci 1988b;40:89–99.

Pascual-Marqui RD. Discrete, 3D distributed, linear imaging methods of electric neuronal activity. Part 1: exact, zero error localization. Math Phys 2007:1–16.

Pearl J. An introduction to causal inference. Int J Biostat 2010;6:7.

Pereda E, Quiroga RQ, Bhattacharya J. Nonlinear multivariate analysis of neurophysiological signals. Prog Neurobiol 2005;77:1–37.

Perrin F, Pernier J, Bertrand O, Echallier JF. Spherical spline for potential and current density mapping. Electroencephalogr Clin Neurophysiol 1989;72:184–7.

Perrin F, Pernier J, Bertrand O, Giard MH, Echallier JF. Mapping of scalp potentials by surface spline interpolation. Electroencephalogr Clin Neurophysiol 1987;66:75–81.

Pezard L, Martinerie J, Breton F, Bourzeix JC, Renault B. Non-linear forecasting measurements of multichannel EEG dynamics. Electroencephalogr Clin Neurophysiol 1994;91:383–91.

Pfurtscheller G, Lopez da Silva F. Event-related EEG/MEG synchronization and desynchronization: basic principles. Clin Neurophysiol 1999;110:1842–57.

Phillips C, Rugg MD, Friston KJ. Systematic regularization of linear inverse solutions of the EEG source localization problem. Neuroimage 2002;17:287–301.

Pijn JP, Velis DN, van der Heyden MJ, DeGoede J, van Veelen CW, Lopes da Silva FH. Nonlinear dynamics of epileptic seizures on basis of intracranial EEG recordings. Brain Topogr 1997;9:249–70.

Premoli I, Castellanos N, Rivolta D, Belardinelli P, Bajo R, Zipser C, et al. TMS-EEG signatures of GABAergic neurotransmission in the human cortex. J Neurosci 2014;34:5603–12.

Principe JC, Brockmeier AJ. Representing and decomposing neural potential signals. Curr Opin Neurobiol 2015;31:13–7.

Riba J, Anderer P, Jané F, Saletu B, Barbanoj MJ. Effects of the South American psychoactive beverage ayahuasca on regional brain electrical activity in humans: a functional neuroimaging study using low-resolution electromagnetic tomography. Neuropsychobiology 2004;50:89–101.

Roehri N, Bartolomei F. Are high-frequency oscillations better biomarkers of the epileptogenic zone than spikes? Curr Opin Neurol 2019;32:213–9.

Rogasch NC, Fitzgerald PB. Assessing cortical network properties using TMS-EEG. Hum Brain Mapp 2013;34:1652–69.

Rosenblum MG, Pikovsky AS, Kurths J. Phase synchronization of chaotic oscillators. Phys Rev Lett 1996;76:1804–7.

Sakkalis V. Review of advanced techniques for the estimation of brain connectivity measured with EEG/MEG. Comput Biol Med 2011;41:1110–7.

Schelter B, Timmer J, Eichler M. Assessing the strength of directed influences among neural signals using renormalized partial directed coherence. J Neurosci Methods 2009;179:121–30.

Schlögl A, Neuper C, Pfurtscheller G. Estimating the mutual information of an EEG-based brain-computer interface. Biomed Tech (Berl) 2002;47:3–8.

Schoffelen JM, Gross J. Source connectivity analysis with MEG and EEG. Hum Brain Mapp 2009;30:1857–65.

Schomer DL, Lopes da Silva FH. Niedermeyer's electroencephalography: basic principles, clinical applications, and related fields. 7th ed. New York: Oxford University Press; 2018.

Schwilden H. Concepts of EEG processing: from power spectrum to bispectrum, fractals, entropies and all that. Best Pract Res Clin Anaesthesiol 2006;20:31–48.

Seeck M, Koessler L, Bast T, Leijten F, Michel C, Baumgartner C, et al. The standardized EEG electrode array of the IFCN. Clin Neurophysiol 2017;128:2070–7.

Seiss E, Hesse CW, Drane S, Oostenveld R, Wing AM, Praamstra P. Proprioception-related evoked potentials: origin and sensitivity to movement parameters. Neuroimage 2002;17:461–8.

Shackman AJ, McMenamin BW, Maxwell JS, Greischar LL, Davidson RJ. Identifying robust and sensitive frequency bands for interrogating neural oscillations. Neuroimage 2010;51:1319–33.

Silber MH, Ancoli-Israel S, Bonnet MH, Chokroverty S, Grigg-Damberger MM, Hirshkowitz M, et al. The visual scoring of sleep in adults. J Clin Sleep Med. 2007;3:121–31.

Shannon CE. A mathematical theory of communication. Bell Syst Tech J 1948;27:623–56.

Sohn H, Kim I, Lee W, Peterson BS, Hong H, Chae JH, et al. Linear and non-linear EEG analysis of adolescents with attention-deficit/hyperactivity disorder during a cognitive task. Clin Neurophysiol 2010;121:1863–70.

Srinivasan R, Winter WR, Ding J, Nunez PL. EEG and MEG coherence: measures of functional connectivity at distinct spatial scales of neocortical dynamics. J Neurosci Methods 2007;166:41–52.

Stam CJ, Nolte G, Daffertshofer A. Phase lag index: assessment of functional connectivity from multi channel EEG and MEG with diminished bias from common sources. Hum Brain Mapp 2007;28:1178–93.

Stam CJ, Pijn JP, Suffczynski P, Lopes da Silva FH. Dynamics of the human alpha rhythm: evidence for non-linearity? Clin Neurophysiol 1999;110:1801–13.

Stam CJ, Reijneveld JC. Graph theoretical analysis of complex networks in the brain. Nonlinear Biomed Phys 2007;1:3.

Stam CJ, van Straaten EC. The organization of physiological brain networks. Clin Neurophysiol 2012;123:1067–87.

Stam CJ. Characterization of anatomical and functional connectivity in the brain: a complex networks perspective. Int J Psychophysiol 2010;77:186–94.

Stam CJ. Nonlinear dynamical analysis of EEG and MEG: review of an emerging field. Clin Neurophysiol 2005;116:2266–301.

Stark J, Broomhead DS, Davies ME, Huke J. Delay embeddings for forced systems: II. Stochastic forcing. J Nonlinear Sci 2003;13:519–77.

Steriade M. Grouping of brain rhythms in corticothalamic systems. Neuroscience 2006;137:1087–106.

Szava S, Valdes P, Biscay R, Galan L, Bosch J, Clark I, et al. High resolution quantitative EEG analysis. Brain Topogr 1994;6:211–9.

Takens F. Detecting strange attractors in turbulence. In: Rand DA, Young LS, editors. Dynamical systems and turbulence, Lecture notes in mathematics 1981;vol. 898. Springer-Verlag; 1981. p. 366–81.

Talairach J, Tournoux P. Co-planar Stereotaxic Atlas of the human brain. New York: Thieme Medical Publishers; 1988.

Teipel S, Grothe MJ, Zhou J, Sepulcre J, Dyrba M, Sorg C, et al. Measuring cortical connectivity in Alzheimer's disease as a brain neural network pathology: toward clinical applications. J Int Neuropsychol Soc 2016;22:138–63.

Theiler J. Spurious dimension from correlation algorithms applied to limited time-series data. Phys Rev A Gen Phys 1986;34:2427–32.

Theiler J, Rapp PE. Re-examination of the evidence for low-dimensional nonlinear structure in the human EEG. Electroencephalogr Clin NeurophysioL 1996;98:213–23.

Theiler J, Eubank S, Longtin A, Galdrikian B, Doyne Farmer J. Testing for nonlinearity in time series: the method of surrogate data. Physica D 1992;58:77–94.

Thomschewski A, Hincapié AS, Frauscher B. Localization of the epileptogenic zone using high frequency oscillations. Front Neurol 2019;10:94.

Valdes PA, Jimenez JC, Riera J, Biscay R, Ozaki T. Nonlinear EEG analysis based on a neural mass model. Biol Cybern 1999;81:415–24.

Valdes-Sosa PA, Roebroeck A, Daunizeau J, Friston K. Effective connectivity: influence, causality and biophysical modeling. Neuroimage 2011;58:339–61.

Valdés-Sosa PA, Vega-Hernández M, Sánchez-Bornot JM, Martínez-Montes E, Bobes MA. EEG source imaging with spatio-temporal tomographic nonnegative independent component analysis. Hum Brain Mapp 2009;30:1898–910.

Van de Steen F, Faes L, Karahan E, Songsiri J, Valdes-Sosa PA, Marinazzo D. Critical comments on EEG sensor space dynamical connectivity analysis. Brain Topogr 2016. https://doi.org/10.1007/s10548-016-0538-7 [Epub ahead of print].

Veiga H, Deslandes A, Cagy M, Fiszman A, Piedade RA, Ribeiro P. Neurocortical electrical activity tomography in chronic schizophrenics. Arq Neuropsiquiatr 2003;61:712–7.

Veth CP, Arns M, Drinkenburg W, Talloen W, Peeters PJ, Gordon E, et al. Association between COMT Val158Met genotype and EEG alpha peak frequency tested in two independent cohorts. Psychiatry Res 2014;219:221–4.

Voytek B, Knight RT. Dynamic network communication as a unifying neural basis for cognition, development, aging, and disease. Biol Psychiatry 2015;77:1089–97.

Waldemar G, Dubois B, Emre M, Georges J, McKeith IG, Rossor M, et al. Recommendations for the diagnosis and management of Alzheimer's disease and other disorders associated with dementia: EFNS guideline. Eur J Neurol 2007;14:1–26.

Wan L, Huang H, Schwab N, Tanner J, Rajan A, Lam NB, Zaborszky L, Li CR, Price CC, Ding M. From eyes-closed to eyes-open: Role of cholinergic projections in EC-to-EO alpha reactivity revealed by combining EEG and MRI. Hum Brain Mapp. 2019;40:566–77.

Wen D, Zhou Y, Li X. A critical review: coupling and synchronization analysis methods of EEG signal with mild cognitive impairment. Front Aging Neurosci 2015;7:54.

Wendling F, Ansari-Asl K, Bartolomei F, Senhadji L. From EEG signals to brain connectivity: a model-based evaluation of interdependence measures. J Neurosci Methods 2009;183:9–18.

Winterer G, Egan MF, Rädler T, Hyde T, Coppola R, Weinberger DR. An association between reduced interhemispheric EEG coherence in the temporal lobe and genetic risk for schizophrenia. Schizophr Res 2001;49:129–43.

Yang Y, Solis-Escalante T, Yao J, Daffertshofer A, Schouten AC, van der Helm FC. A general approach for quantifying nonlinear connectivity in the nervous system based on phase coupling. Int J Neural Syst 2016;26:1550031.

Yao D, He B. A self-coherence enhancement algorithm and its application to enhancing three-dimensional source estimation from EEGs. Ann Biomed Eng 2001;29:1019–27.

Yao D, Wang L, Arendt-Nielsen L, Chen AC. The effect of reference choices on the spatio-temporal analysis of brain evoked potentials: the use of infinite reference. Comput Biol Med 2007;37:1529–38.

Yao D. A method to standardize a reference of scalp EEG recordings to a point at infinity. Physiol Meas 2001;22:693–711.

Yuval-Greenberg S, Tomer O, Keren AS, Nelken I, Deouell LY. Transient induced gamma-band response in EEG as a manifestation of miniature saccades. Neuron 2008;58:429–41.

Z-Flores E, Trujillo L, Sotelo A, Legrand P, Coria LN. Regularity and Matching Pursuit feature extraction for the detection of epileptic seizures. J Neurosci Methods 2016;266:107–25.

Ziemann U. Transcranial magnetic stimulation at the interface with other techniques: a powerful tool for studying the human cortex. Neuroscientist 2011;17:368–81.